	<b>CHAMP Magnetic Test Report</b>	Doc: CH-GFZ-TR-2000 Issue: 1.0 Date: 15.06.2000 Page: 1 of 51
---	---------------------------------------	--


## CH-GFZ-TR-2000

# CHAMP Magnetic Test Report

	Name	Date and Signature
Prepared by:	H. Lühr, R. Bock, M. Rother	<i>R. Bock, M. Rother</i>
Checked by:	Prof. Dr. H. Lühr	19.6.00 <i>H. Lühr</i>
Project Management:	Prof. Dr. Dr. Ch. Reigber	20/6/00 <i>Ch. Reigber</i>

**Document Change Record**

Issue	Date	Page	Description of Change
1.0	15.06.00	all	First Issue

	<b>CHAMP Magnetic Test Report</b>	Doc: CH-GFZ-TR-2000 Issue: 1.0 Date: 15.06.2000 Page: 3 of 51
---	---------------------------------------	--

## SUMMARY OF RESULTS

This report comprises the results of the CHAMP DC Magnetic System Test. The test was performed at the magnetic field test facility (MFSA) of the IABG in Ottobrunn, Germany. Since CHAMP is intended to be a magnetic field reference mission, the magnetic properties of the spacecraft may directly influence the quality of the returned measurements. For that reason this test is not only used for verifying the compliance of the spacecraft (S/C) with the magnetic cleanliness specification but also reveals important features for the scientific mission.


Some major results of the tests are:

- The magnetic moment of the S/C is  $<1\text{Am}^2$ .
- The S/C-related magnetic field (remanent and induced) is  $<1\text{nT}$  at the OVM and has been modeled.
- Stray fields of electrical currents (except for thrusters and torquers) are  $<0.1\text{nT}$  at FGM 1.
- The torquer-related disturbances have been calibrated.
- The system performance of the torquers has been checked and found to be about 5% below specification.
- The relative orientation of the FGMs with respect to the S/C coordinates has been determined.
- The non-linearity coefficients of the FGMs have been verified.
- Finally the precise dating of the magnetic readings wrt. an absolute clock (GPS time) has been verified.

As a by-product of this test, three close-loop AOCS simulation runs could successfully be performed. A magnetic environment as to be expected in orbit was generated by the magnetic facility.

There is one item which could not be tested, namely the magnetic disturbances emanating from the currents through the solar cell strings. An investigation of that effect can only be done properly in space. Related measurements should be made with both FGMs in the stowed and the deployed boom configuration.

In summary, it can be stated that the spacecraft is compliant with the stringent magnetic cleanliness requirements. Together with the demonstrated high performance of the instruments of the magnetometry package, the CHAMP mission promises to return magnetic field measurements of unprecedented quality.


	<b>CHAMP Magnetic Test Report</b>	Doc: CH-GFZ-TR-2000 Issue: 1.0 Date: 15.06.2000 Page: 4 of 51
---	---------------------------------------	--

## LIST OF CONTENTS

<b>1</b>	<b>SCOPE .....</b>	<b>6</b>
	1.1 Test Objectives.....	6
	1.2 Test Specimen.....	6
	1.3 Test Date and Location .....	6
<b>2</b>	<b>DOCUMENTS .....</b>	<b>7</b>
<b>3</b>	<b>TEST CONDITIONS .....</b>	<b>7</b>
	3.1 Facility and Instrumentation .....	7
	3.2 Test Conditions.....	7
<b>4</b>	<b>TEST SETUP .....</b>	<b>9</b>
	4.1 Configurations for Magnetic Field Tests .....	9
<b>5</b>	<b>SEQUENCE OF TEST STEPS .....</b>	<b>14</b>
<b>6</b>	<b>MAGNETIC PROPERTIES OF THE SPACECRAFT.....</b>	<b>15</b>
	6.1 Remanent Magnetization.....	15
	6.2 Induced Magnetization .....	16
<b>7</b>	<b>STRAY FIELD OF ELECTRICAL CURRENTS, BOOM STOWED.....</b>	<b>17</b>
	7.1 Instrument Switch-on Sequence .....	18
	7.2 Switching AOCS Components.....	23
	7.3 Switching the Heaters.....	28
<b>8</b>	<b>STRAY FIELD, BOOM DEPLOYMENT.....</b>	<b>31</b>
	8.1 Switch on of Instruments .....	31
	8.2 Switching AOCS Component.....	31
<b>9</b>	<b>PROPERTIES OF THE MAGNETORQUERS .....</b>	<b>34</b>
	9.1 Stowed Boom Configuration .....	34
	9.2 Deployed Boom Configuration .....	35
	9.3 Timing of the Torquer Control .....	37
	9.4 Performance of the Torquers.....	40
<b>10</b>	<b>ORIENTATION OF THE FGMs .....</b>	<b>40</b>
	10.1 FGM Transformation Matrices for AOCS.....	40
	10.2 FGM Transformation Matrices for Science Application.....	41

**11 CHARACTERISTICS OF THE MAGNETOMETERS ..... 43**

- 11.1 Non-Linearity Coefficients of the FGMs ..... 43**
- 11.2 Calibration of the Coil Facility ..... 44**
- 11.3 Vector-Calibration of the FGMs ..... 44**
- 11.4 Scalar Calibration of the FGMs..... 47**
- 11.5 Characteristics of the OVM ..... 47**
- 11.6 Timing of the Magnetic Field Readings ..... 49**

	<b>CHAMP Magnetic Test Report</b>	Doc: CH-GFZ-TR-2000 Issue: 1.0 Date: 15.06.2000 Page: 6 of 51
---	---------------------------------------	--

## 1 SCOPE

This document gives a test report of the system magnetic test of the CHAMP spacecraft at the magnetic facility of the IABG. It contains all the test results and derived quantities obtained during the operation of the spacecraft bus and payload instruments in an magnetically defined environment.

The demand on the quality of this test was very high. CHAMP as a magnetic field mapping mission requires absolute accuracy for its magnetometers, not perturbed by the spacecraft. Omitted or wrong corrections of the measurements will directly enter the field models.

### 1.1 Test Objectives

The prime objective of this test was to verify that the CHAMP spacecraft meets the stringent magnetic requirements imposed on it by the special scientific goals of the mission. Secondary objectives were the determination and verification of the characteristics of the magnetic AOCS sensors and actuators as well as testing the properties of the magnetometers on system level. Of particular interest are:

- a) The magnetic properties of the spacecraft
- b) The magnetic disturbances generated by the power system
- c) The radiated AC magnetic noise
- d) The magnetic properties of the torquers
- e) The orientation of the FGMs with respect to spacecraft coordinates.
- f) The characteristics of the magnetometers

### 1.2 Test Specimen

The item to be tested was the CHAMP spacecraft in a near-flight configuration. Deviations from flight configuration (e.g. missing solar panels) are listed in [RD 01] and [RD 02].


### 1.3 Test Date and Location

Date: 5-11 February 2000

Location: Industrieanlagen Betriebsgesellschaft mbH (IABG), Ottobrunn, Germany

Facility: Magnetfeld-Simulationsanlage (MFSA)

geogr. coordinates: Latitude: 48.0385°N  
Longitude: 11.665°E  
Altitude: 670 m

	<b>CHAMP Magnetic Test Report</b>	Doc: CH-GFZ-TR-2000 Issue: 1.0 Date: 15.06.2000 Page: 7 of 51
---	---------------------------------------	--

## 2 DOCUMENTS

- [RD 01] "CHAMP Magnetic Test Procedure",  
CH-GFZ-TP-2000 issue 1.1
- [RD 02] "Vorbereitung CHAMP Magnettest", minutes of meeting CH-GFZ-MM-66  
"Vorbereitung CHAMP Magnettest (2)", minutes of meeting CH-GFZ-MM-68  
"CHAMP Magnetic Test Readiness Review", minutes of meeting CH-GFZ-MM-74
- [RD 03] "Magnetic Calibration of the CHAMP Boom Instrumentation",  
CH-GFZ-TR-2602 issue 1.1
- [RD 04] "CHAMP Mission and system requirements Specification",  
CH-GFZ-SP-0001 issue 2.4
- [RD 05] "Magnetic Test Facilities", part of IABG test facility description  
TN-TR-1000 issue 08/98
- [RD 06] "Magnetic Test", B-TR-40-0398, IABG Test Report
- [RD 07] "Overhauser Magnetometer Performance Test Report",  
CH-GFZ-TR-2501 issue 1.0

## 3 TEST CONDITIONS

### 3.1 Facility and Instrumentation

The measurements were performed in the magnetic test facility (MFSA) of the IABG. In the center of the system the Earth's field and its variations are compensated automatically. Artificial fields up to 80000 nT in any direction can be generated by the coils. The field settings may either be selected by computer control or by the input of analogue control voltages. The latter was intensively used for the AOCS closed-loop test runs. Further details of the coil facility can be found in [RD 05].

For monitoring the field distribution outside the CHAMP spacecraft, especially during tests when the S/C was not powered, readings of the Förster fluxgate magnetometers (FM1, FM2, FM3, FM4) were used. These magnetometers are part of the facility monitoring system. Repeatedly FM1 delivered bad readings. These outliers could easily be detected and thus did not deteriorate the results.

### 3.2 Test Conditions

The temperature is a parameter which influences the characteristics of the system (e.g. thermal expansion of the coils). From previous measurement [RD 03] it is known that the scale factor for example is decreasing by some 23 ppm per degree. With the help of 9 thermistors well distributed in the facility we get a good overview of the temperature field in the facility. Figure 3.2-1 shows the recorded temperature at three representative positions. The close thermal control provides a stable environment at a temperature of  $18.6^{\circ} \pm 0.3^{\circ}\text{C}$ .

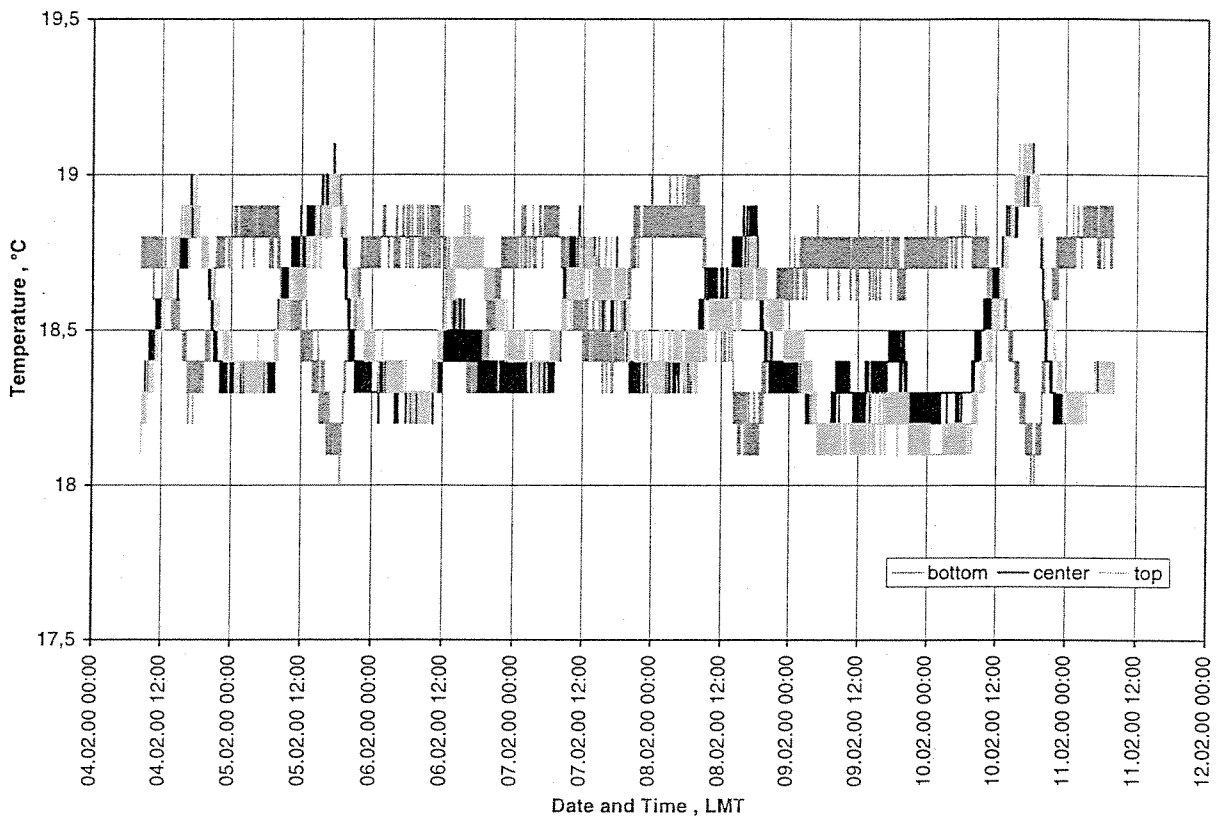


Figure 3.2-1 Air temperature in the MFSA (coil SW) during the CHAMP Magnetic System Test

Another relevant quantity is the prevailing geomagnetic activity which may enhance the noise floor in the system. Fortunately, the activity was only moderately disturbed during the test period as can be seen from the below listed Kp indices of the relevant days. A somewhat higher activity (Kp = 4 to 5) was encountered on Sunday, Feb. 6 when no measurements were made and on Monday, Feb. 7 when only measurements with the stowed boom were performed which are less sensitive.

YYMMDD	Kp-Index								SUM
000205	1o	0+	0+	1o	1o	3o	4+	4+	15+
000206	5-	5o	4-	4+	4o	3+	5-	5o	35-
000207	5+	4-	4-	4o	5-	4o	4o	4o	33+
000208	4-	3+	2-	3-	3o	3o	4-	3-	24-
000209	2-	3o	3-	1+	3o	4-	2o	2-	19o
000210	3-	2+	3o	2-	2o	2+	2o	3+	19+
000211	3o	4+	3-	3-	2+	3o	3-	4+	25o

An indicator for the stability of the facility and the magnetic environment is the zero field in the center of the facility. This quantity has been measured repeatedly during the test period. Table 3.2-1 lists the obtained values.



*Table 3.2-1 Temporal behavior of the zero field in the facility center*

Date and Time (CET)		West	North	Down	Sensor
		nT	nT	nT	bias
5.2.00	12:30	3.85	-28.9	-5.75	-1.37
5.2.00	14:40	4.4	-28.55	-5.8	-1.3
5.2.00	18:20	5.5	-28.55	-4.7	-2.8
7.2.00	09:50	5.15	-29.25	-4.95	-2.5
9.2.00	19:30	6.03	-28.97	-4.50	na (OVM)

In the north component we find a somewhat elevated value. This is probably due to the large amount of electrical test equipment in the facility entrance hall. Since the equipment was not moved around, the offset value is rather constant.

It was decided not to adjust the zero field in the facility, but rather compensate for it in the post-processing. The observed drift of about 1 nT over the week causes no problems for the executed measurements.

## 4 TEST SETUP

### 4.1 Configurations for Magnetic Field Tests

The ambitious objectives of this test required a dedicated selection of the test set-up. As a prerequisite, all magnetic items had to be kept away from the test specimen as far as possible. For that reason the whole satellite checkout equipment (CCS, EGSEs etc.) was installed in the MFSA entrance hall some 20 m to the north of the facility center. Figure 4.1-1 gives an overview of the locations of the major test items. For the various test steps the spacecraft had to be placed at dedicated positions. The S/C center of gravity positions labeled RP1 through RP5 are also marked in Figure 4.1-1.

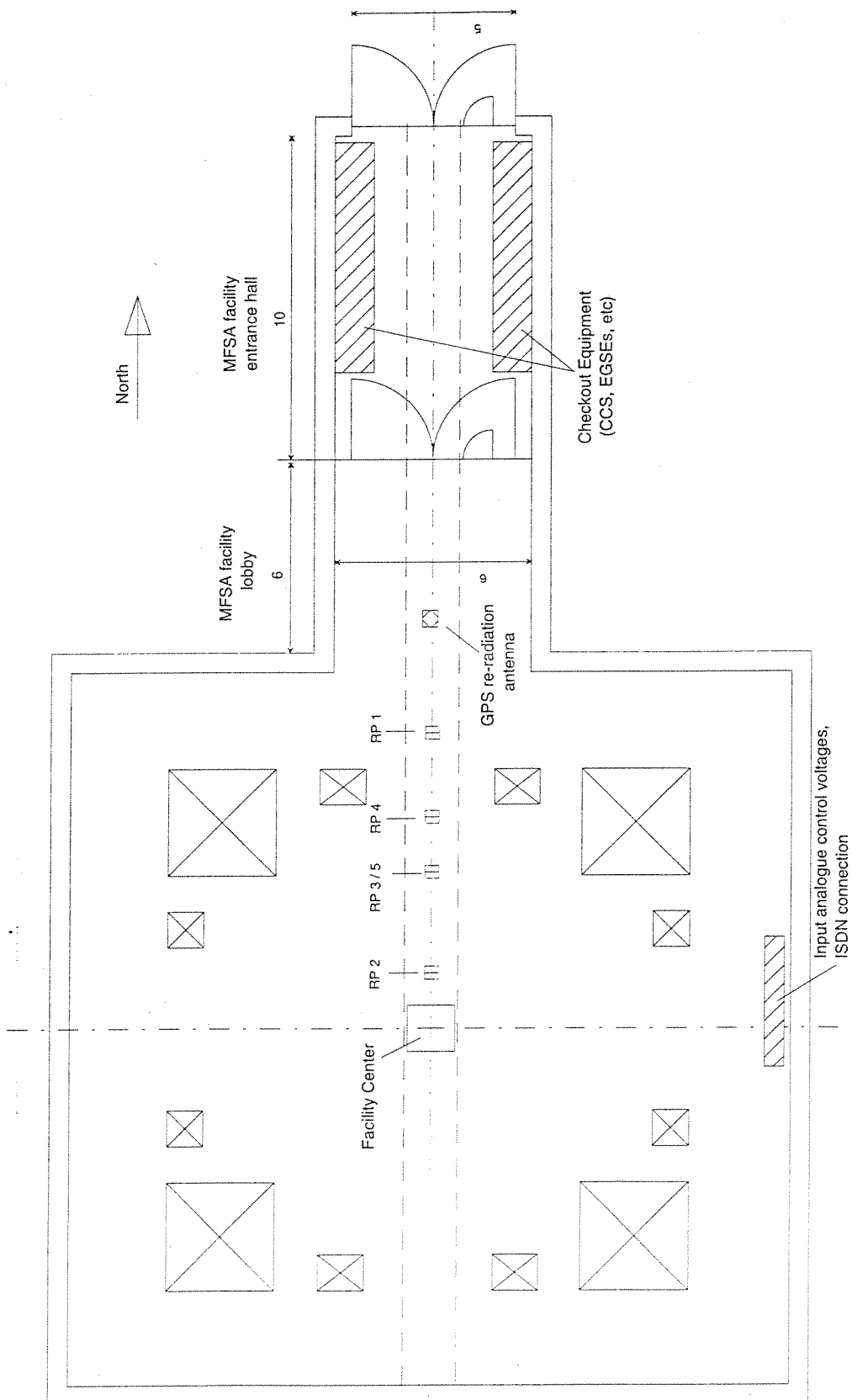


Figure 4.1-1 Overview of test item locations in the MFSA facility

The CHAMP satellite was placed on the turntable of the non-magnetic facility trolley. In Figure 4.1-2 the relative position of the spacecraft flight CoG to the trolley rotation axis and the facility floor is given. These numbers are important for the identification of spacecraft units with respect to detected disturbance dipoles.

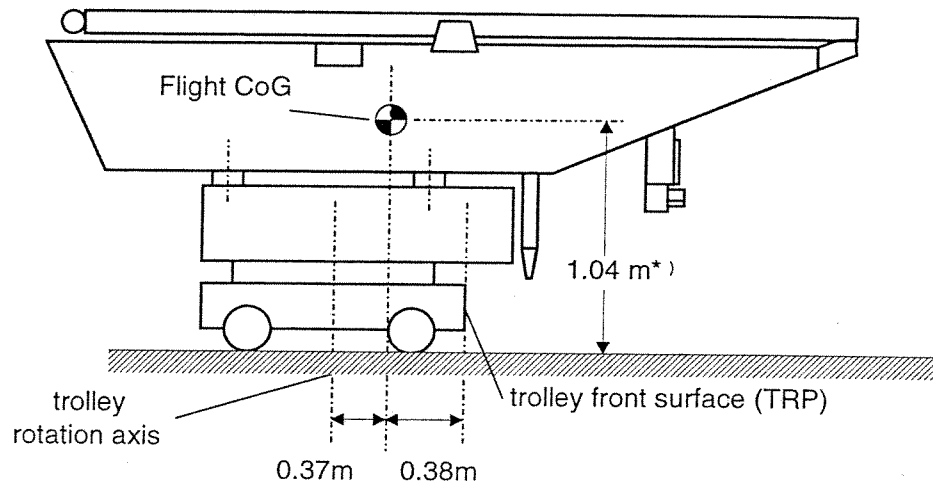


Figure 4.1-2 Position of trolley reference point wrt. flight CoG (Accelerometer Sensor) and trolley rotation axis

\* During the test it turned out that the height of the CoG was 3 cm lower than planned. For this reason numbers reflecting the height of satellite items in this and subsequent figures have actually been lower by 3 cm.

The test configuration for all runs with the passive spacecraft and for the stray fields with the boom stowed is depicted in Figure 4.1-3.

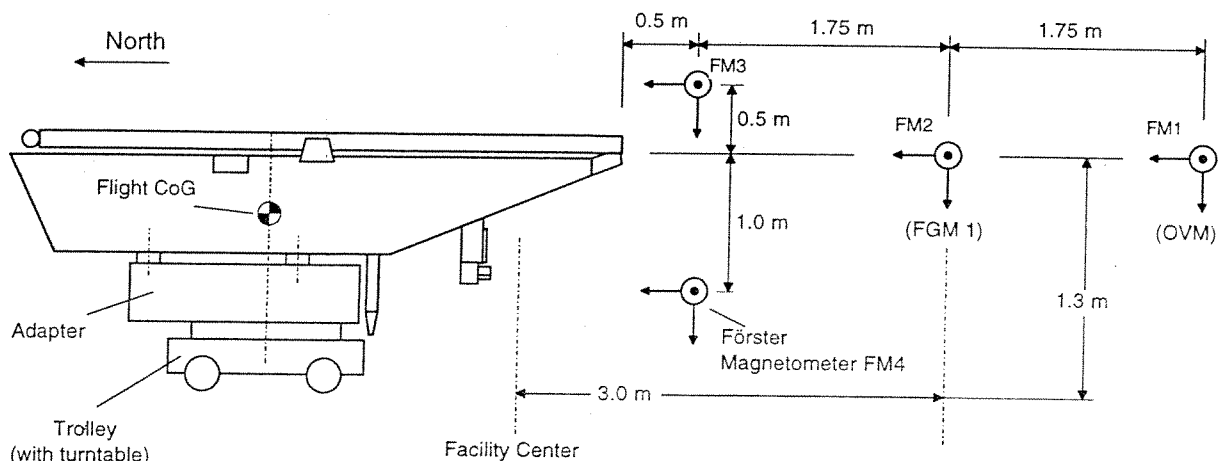


Figure 4.1-3 Test set-up for the test steps 6.4 and 6.5 (boom stowed)

Coordinate assignment for Figure 4.1-3:

FGM 1 / 2	Facility
X	North
Y	West
Z	Up

Figure 4.1-4 shows the set-up for the measurements with the boom deployed. Great care was taken that the dip angle of the boom ( $1.8^\circ$  below horizontal) was as close as possible to the flight configuration. Furthermore, the alignment of the S/C axes wrt. the facility axes was adjusted with the help of a laser pointer to better than  $0.1^\circ$ .

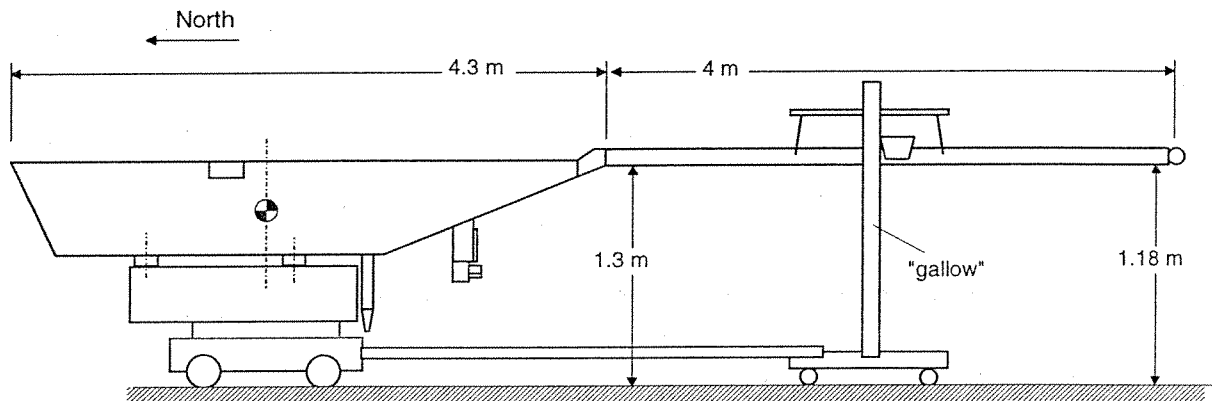


Figure 4.1-4 Test set-up for the test steps 6.6 and 6.7 (boom deployed)

Coordinate assignment for Figure 4.1-4:

FGM 1 / 2	Facility
X	South
Y	West
Z	Down

For the very low level AC magnetic field measurements the low-frequency search coil sensor was placed in the center of the facility to ensure lowest contamination from the environment. The distance to the spacecraft was chosen such that the AC sensor was at the position of the FGM1 deployed boom configuration. The specification of the noise spectrum in [RD 04] is valid for the position of FGM1.

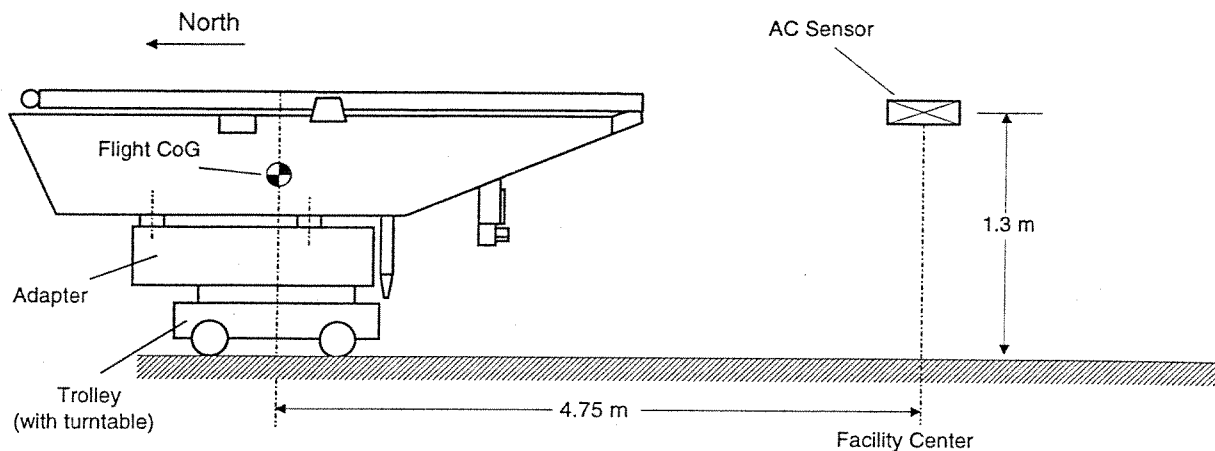


Figure 4.1-5 Test set-up for measuring the AC magnetic radiation


Table 4.1-1 lists all the used reference points. We will refer to these RPs in the various sections of this report.

Table 4.1-1 Reference Points in the MFSA

Point	X [m] *	Description
RP 1	9.05	CHAMP is out of the coil system near the facility lobby; position used for calibration and zero-field verification of the facility (reference measurements)
RP 2	1.37	FGM1 is 3.00 m out of facility center; CoG is 1.75 m out of facility center
RP 3	4.37	FGM1 is in the facility center
RP 4	6.12	OVM is in the facility center
RP5	4.37	Satellite CoG is 4.75 m north of facility center (for AC magnetic measurements). The AC sensor is in the facility center. (Same as RP3)

\* Trolley reference Point (TRP= with respect to the facility center; in +North-direction)

During measurements with active instruments the satellite was powered by an external battery located some 20 m away, in the facility entrance hall. This deviation from flight configuration was tested wrt. magnetic effects. No response could be detected at the location of the boom mounted payload instruments.

	<b>CHAMP Magnetic Test Report</b>	Doc: CH-GFZ-TR-2000
		Issue: 1.0
		Date: 15.06.2000
		Page: 14 of 51

## 5 SEQUENCE OF TEST STEPS

The DC Magnetic Test was conducted as outlined in the test procedure [RD 01]. In this section we will list the dates and times when the individual test steps have been performed. See also chapter 6 in the filled-in test procedure [RD 01]. The times listed below represent the approximate start of the test step. The system time refers to the on-board time which is derived from the GPS time information.

Test step	Date	Local Time (LMT or UTC)	System Time (GPS seconds)	Remarks / Data File
<b>6.2 Remanent Field of Spacecraft</b>				
6.2.2	05.02.00	11:25 LMT	n.a.	Facility reference measurement (file CHAMP 002)
6.2.3	05.02.00	11:10 UTC	n.a.	Remanent field measurement (file CHAMP 003)
6.2.1	05.02.00	12:30 LMT	n.a.	Zero field verification
<b>6.3 Induced Magnetic Field of Spacecraft</b>				
6.3.1	05.02.00	14:40 LMT	n.a.	Zero field verification
6.3.2	05.02.00	15:29 LMT and 16:53 LMT	n.a.	Induced magnetic field measurement. Settings acc. to file: RAND_64.SET (files CHAMP 005 and CHAMP 006)
6.3.3	05.02.00	18:20 LMT	n.a.	Facility reference measurement (file CHAMP 007)
<b>6.4 Stray Field of Currents (boom stowed)</b>				
6.4.2	07.02.00	9:50 LMT	n.a.	Zero field verification
6.4.3	07.02.00	11:30 LMT	n.a.	Stray Field measurement, boom stowed
6.4.3.6 - 6.4.3.25	07.02.00	11:36 LMT	~ 633 955 666	Payload switch-on sequence (file CHAMP 010)
additional	07.02.00	13:46 LMT	~ 633 963 686	Repeat Payload switch-on sequence
6.4.3.26 - 6.4.3.35	07.02.00	13:02 UTC	~ 633 963 747	Switching AOCS components and heaters. TC-file: "MAG_TEST_RUN:_1.ODL"
6.4.3.36 - 6.4.3.59	07.02.00	15:50 UTC	~ 633 973 916	Switching redundant components (file CHAMP 012)
6.4.4	07.02.00	17:57 LMT	n.a.	FGM orientation measurement. TC-file: "MAG_TEST_STOWED.ODL"
<b>6.5 AC Magnetic Test <sup>1)</sup></b>				
6.5.1	08.02.00	09:14 UTC	n.a.	AC Magnetic Test. TC-file: "MAG_TEST_AC.ODL"
<b>6.6 Boom Deployment</b>				
6.6.3	08.02.00	17:20 UTC	~ 634 066 380	Timing and Synchronization Test. TC-file: "MAG_TEST_TIMING.ODL"
6.6.4	08.02.00	19:17 UTC	~ 634 067 276	Payload Switch-Off Sequence Test
<b>6.6.2 Stray Field of Currents (boom deployed)</b>				
6.6.2.6 - 6.6.2.16	09.02.00	08:20 UTC	n.a.	Payload switch-on sequence
6.6.2.17 - 6.6.2.25	09.02.00	09:06 UTC	~ 634 122 360	Switching AOCS components and heaters. TC-file: "MAG_TEST_RUN:_2.ODL"
6.6.2.26 - 6.6.2.41	09.02.00	09:48 UTC	~ 634 124 914	Switching redundant components
additional	09.02.00	10:36 UTC	~ 634 127 832	OVM-Switching Influence on FGM1 Test

**GFZ**

POTSDAM

**CHAMP Magnetic Test  
Report**

Doc: CH-GFZ-TR-2000

Issue: 1.0

Date: 15.06.2000

Page: 15 of 51

Test step	Date	Local Time (LMT or UTC)	System Time (GPS seconds)	Remarks / Data File
6.7 Boom Attitude / Boom Flexing				
6.7.3	09.02.00	12:49 UTC	~ 634 135 740	Torquer Influence on OVM Test. TC-file: "MAG_TEST_BOOM.ODL"
6.7.4	09.02.00	13:47 UTC	~ 634 143 924	Linearity Check. Settings: LIN_X , LIN_Y , LIN_Z
additional	09.02.00	15:20 UTC	n.a.	MMU dump
6.7.5	09.02.00	15:49 UTC	~ 634 147 100	Boom Attitude Measurement. Settings: THIN_50
additional	10.02.00	07:35 UTC	n.a.	OVM Test (reaction on OBDH switch-over)
6.8 (1.1)	10.02.00	08:48 UTC	*) n.a.	AOCS FPM and MMU dump
6.8 (1.3)	10.02.00	13:51 UTC	*) n.a.	AOCS FPM slew maneuver
additional	10.02.00	15:28 UTC	*) ~ 641 156 600	ACC coil activation test (system time driven by preceding AOCS slew test)
6.8 / additional	10.02.00	15:40 UTC	*) ~ 641 157 320	AOCS torquer spike test (AOCS fine pointing mode simulation with torquer control)
additional	11.02.00	09:35 LMT and 10:21 LMT	n.a.	Y-torquer performance test. (files CHAMP 027 and CHAMP 029)
6.8 (1.1)	11.02.00	09:40 UTC	*) n.a.	AOCS RDM (boom stowed) and MMU dump

<sup>1)</sup> The results of the AC Magnetic Test are presented in "CHAMP EMC Test Report" (CH-IT-TR-2002)

\*) The on-board system time depends on the AOCS simulation mode because also the GPS time information is simulated by the AOCS SCOE. These times noted here were scheduled for a satellite launch on April 28.

## 6 MAGNETIC PROPERTIES OF THE SPACECRAFT

The magnetic properties of the test specimen comprise its remanent magnetization and the influence of the soft magnetic material here called induced magnetization.

### 6.1 Remanent Magnetization

For the determination of the remanent magnetization of CHAMP the spacecraft was rotated in front of a series of Förster magnetometers as depicted in Figure 4.1-3. Measurements were taken at 10° intervals. At 0° the forward end of CHAMP pointed south, at 90° towards west, at 180° towards north and at 270° towards east.

The readings of the Förster magnetometers FM1 through FM4 were modeled to identify equivalent dipoles which could account for the field distribution observed in the vicinity of the CHAMP spacecraft. A detailed description of the observations and the model results are given in [RD 06] of which only some relevant facts are quoted here.

A minimum number of three disturbance dipoles is needed to achieve a satisfying match between model and observation. Therefore we will only consider this case in the following assessment. The obtained locations in the S/C (taking into account the 3 cm mismatch) and the magnetic moments are:

Table 6.1-1: Position and magnetic moment of disturbance dipoles

Dipole #	Position [mm]			magn. Moment [mA m <sup>2</sup> ]			
	X	Y	Z	M <sub>x</sub>	M <sub>y</sub>	M <sub>z</sub>	M <sub>total</sub>
1.	-517	76	57	15	-1532	1202	1947
2.	535	-5	9	72	1471	-422	1532
3.	1079	49	-315	-110	-38	221	250

A comparison of the equivalent dipoles with the accommodated units in CHAMP reveals a reasonable fit with the CoGs of the following components:

Component	CoG Position [mm]		
	X	Y	Z
aft cold gas tank	-532	0	0
forward cold gas tank	532	0	0
OBDH unit	1171	0	-41

These three units can account for about 90% of the overall observed magnetic moment. The unexpectedly height moments of the tanks cancel each other quite effectively due to their accommodation. The resulting total dipole moment of the spacecraft amounts to about 1 Am<sup>2</sup> and is pointing almost entirely into the S/C z direction. The magnetic bias expected from this field at the OVM is about 0.35 nT.

When considering also later measurements (e.g. induced magnetization, FGM readings in stowed configuration) consistent results are obtained for the estimated moment of M<sub>y</sub>. The fairly large M<sub>z</sub> components, however, could not be confirmed. A revision of the data taken showed that the discrepancy is not caused by wrong measurements or interpretation. The spacecraft must have changed its magnetic moment after the first test step. The new dipole moment is less than 0.5 Am<sup>2</sup> and is well distributed among the three components.

The remanent magnetic field of the spacecraft can be considered in the OVM data processing. The correction procedure should look like


$$B = B_{OVM} - \frac{XX_o + YY_o + ZZ_o}{B_{OVM}} \quad (6.1-1)$$

where X, Y, Z are the FGM readings in S/C coordinate system and X<sub>o</sub> = 0, Y<sub>o</sub> = -0.3 nT and Z<sub>o</sub> = 0 are the recommended CHAMP biases.

## 6.2 Induced Magnetization

For the determination of the induced magnetic field of the spacecraft, 82 different facility field settings with a constant amplitude of 64000 nT but randomly distributed directions have been applied. The first set of measurements was made with the satellite at RP1 (out of the facility) and a second, identical run was performed with the spacecraft at RP2. By comparing the two



	<b>CHAMP Magnetic Test Report</b>			Doc: CH-GFZ-TR-2000
				Issue: 1.0
				Date: 15.06.2000
				Page: 17 of 51

data sets the modification caused by the spacecraft can be determined. Below we list the results obtained at the four facility magnetometers FM1 through FM4 (cf. Figure 4.1-3).

*Table 6.2-1: Modification of magnetic field due to soft magnetic parts in the spacecraft*

	Influence on scale factor			Magnetic bias [nT]			Angular distortion [arc sec]		
	West	North	Down	West	North	Down	(W,N)	(W,D)	(N,D)
FM1	1.000006	0.9999845	1.000005	-0.31	0.13	-0.01	0	1	1
FM2	1.000013	0.9999647	1.000015	-1.04	0.04	-0.54	0	0	1
FM3	1.000076	0.9998744	1.000049	-4.10	3.11	-3.25	-1	1	28
FM4	1.000066	0.9998835	1.000050	-4.66	-1.65	-1.38	0	0	-21

When discussing the listed results we pay special attention to readings of FM1 and FM2, since they reflect the effects at OVM and FGM1, respectively. There is a clear influence on the scale factor (values above 1 indicate a weakening of the field). Consistently we find an amplification of the field in North/South direction, along the S/C x axis and a weakening for the two perpendicular components. This is consistent with pulling the magnetic field lines into the soft magnetic parts (the tanks) of the spacecraft. At the location of the OVM the scale factor is modified by 15 ppm resulting in a misreading of 0.9 nT at a field strength of 60000 nT. The specification in [RD 04] requires an effect of less than 1 nT which is just met.

The magnetic bias reflects the remanent magnetic effect which has been discussed in the previous section. The distortion of the field direction is negligible at FM1 and FM2. The deflection of the field lines in the North/Down plane indicated in the results of FM3 and FM4 nicely confirm the suggested pulling of the magnetic field lines into the spacecraft body.

For the mission data processing it is proposed to correct the observed modification of the field strength (scale factor) as part of the OVM data processing. The correction procedure should look like


$$B = B_{OVM} - (14 \cdot 10^{-6} \cdot X^2 - 6 \cdot 10^{-6} \cdot Y^2 - 5 \cdot 10^{-6} \cdot Z^2) / B_{OVM} \quad (6.2-1)$$

where X, Y and Z are the magnetic field components in S/C coordinates derived by FGM.

## 7 STRAY FIELD OF ELECTRICAL CURRENTS, BOOM STOWED

An important part of the magnetic cleanliness of a spacecraft is the stray field caused by electric currents flowing in the power lines and in the instruments. During the design of the spacecraft special attention was paid to this requirement. Some of the means to achieve a magnetically clean satellite, which were applicable for CHAMP, are self-compensating power lines and a single point grounding concept.

We performed a full sequence of stray field measurements with the boom stowed although this is not a nominal operational configuration. The advantage of measurements in this configuration is the proximity of the fluxgate sensors FGM1 and FGM2 to the disturbing sources. With the help of the two-point measurement we could affiliate a stray field magnetic moment to each of the active units. This gives us the possibility to predict the expected perturbation at the location of the magnetometers in the deployed configuration.

	<b>CHAMP Magnetic Test Report</b>	Doc: CH-GFZ-TR-2000 Issue: 1.0 Date: 15.06.2000 Page: 18 of 51
---	---------------------------------------	---

The test set-up used for this sequence is shown in Figure 4.1-3, where the spacecraft is positioned at reference point RP2. The Förster magnetometers FM1 through FM4 were also operated taking two readings per test step. The purpose of these external test points was (a) to get an idea of the magnetic differences between a passive and a powered spacecraft and (b) to be able to distinguish between electrical interferences and magnetic perturbations of the FGMs emanating from other units.

## 7.1 Instrument Switch-on Sequence

During the first sequence of this test step the spacecraft was powered up and the instruments switched on. Between the switchings readings were taken by the onboard FGMs and the Förster magnetometers. The first power-up of the satellite (activating PCPU, RFEA, OBDH and FGM1) caused no noticeable magnetic effect ( $<0.5$  nT) even at the nearby external sensors FM3 and FM4. For the subsequent switchings measurements of the FGMs are available. Figure 7.1-1 shows the response of the FGMs to the power-up of the instruments. Only a few events stick out of the noise of about 0.5 nT in the facility. For a more quantitative overview the magnetic responses in nT at the two FGMs are listed in Table 7.1-1.

As a general remark, we find a harmonic disturbance signal at a period of some 16 sec with an amplitude of about 0.5 nT in the FGM 2 Y component. This signal is persistently present in all recordings which were taken in the stowed boom configuration. With the help of the dual magnetometer method we spot the source in the OBDH. The only cyclic activity variation at a 16 sec period which comes to our mind, is the AOCS thruster control (16 sec inhibit time).

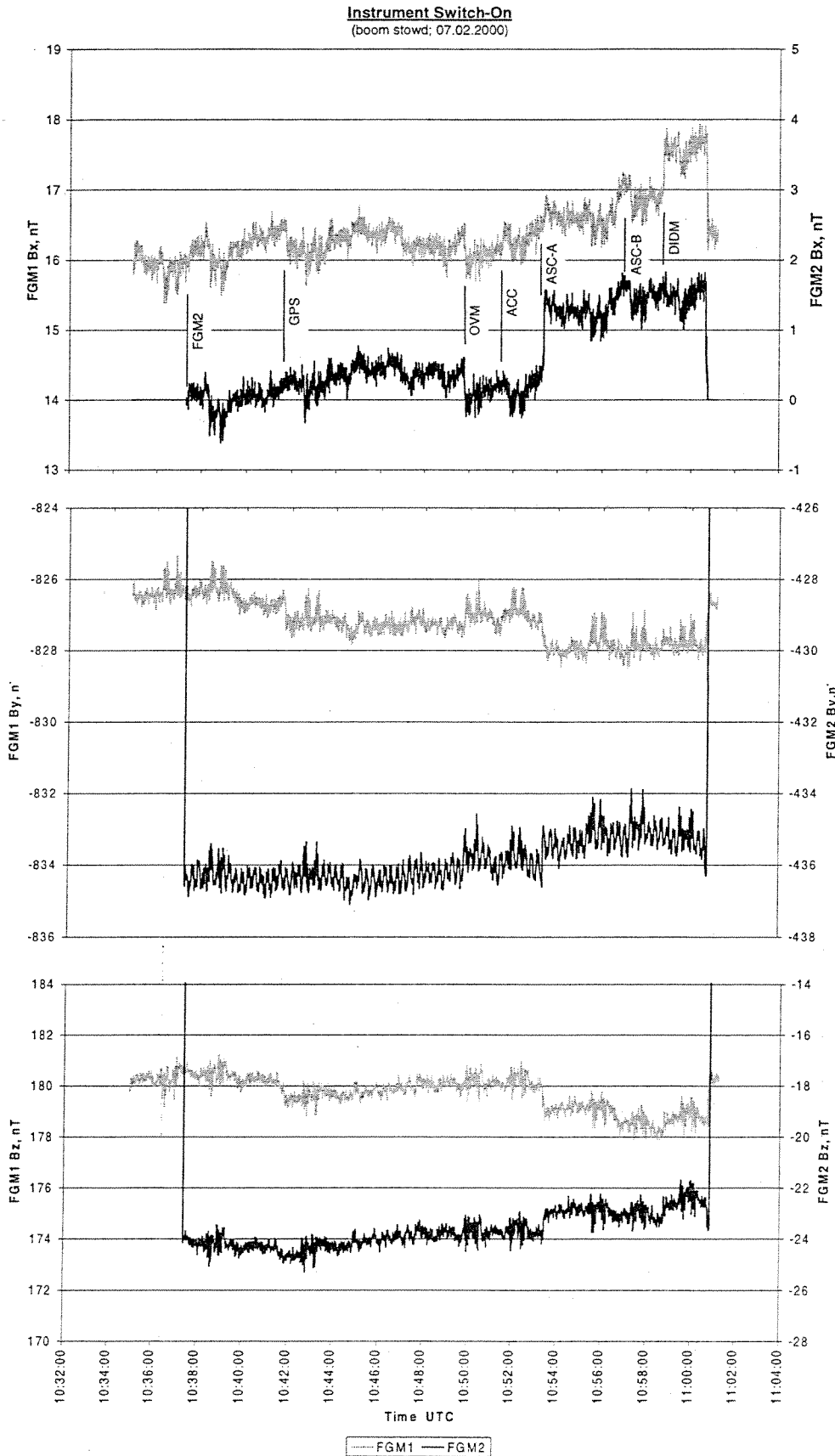


Figure 7.1-1 FGM 1 and 2 response to instrument switch-on , boom stowed

*Table 7.1-1: Magnetic disturbances causes by payload instruments, boom stowed*

Instrument	FGM 1			FGM2		
	dX	dY	dZ	dX	dY	dZ
FGM2	0	0	0	na	na	na
GPS_M	-0.3	-0.5	-0.6	0	0	0
OVM	-0.2	0	0	-0.2	0	0
ACC_1	0	0	0	0	-0.2	0
ASC_A	0.2	-0.9	-0.8	1.0	0.2	0.6
ASC_B	0.2	0	-0.5	0	0	0
DIDM	0.7	0	0.4	0	0	0.3
All off	-1.2	1.5	1.6	na	na	na

From the above table and figures it is evident that the perturbations are larger at FGM1 than at FGM2. This is due to the smaller separation of FGM1 to most of the electronics boxes. In the stowed configuration the locations of the two magnetometers are (0.354 m; 0 m; -0.482 m) for FGM1 and (0.954 m; 0 m; -0.482 m) for FGM2 in the spacecraft coordinate system with respect to the flight CoG. Since the disturbances are generally below 1 nT, no magnetic effect from the instruments is expected in the deployed configuration. An exception is the observed response of FGM2 to ASC\_A. This effect is known from previous tests [RD 03] and is caused by the ASC\_A sensor cables that are routed close to the FGM2 sensor. The listed deflections reflect the worst case, since both camera heads were overexposed.

The critical units on-board CHAMP have redundant components. For completeness we also investigated the magnetic effect of switching over to them. Figure 7.1-2 shows the magnetic deflections recorded during this part of the test. During the first interval on Figure 7.1-2 all instruments are running with their main components. The subsequent data gap is caused by the switch of the OBDH from Main to Redundant. After this boot-up all payload instruments had to be switched on again. This is reflected by the step-like change following the gap. Comparing the readings from the beginning of this test step with those when the spacecraft is fully operational again after switching to the redundant OBDH, we note a level shift in all components of the FGM2 (dX = -1nT, dY = -2nT, dZ = -4nT). The confinement of the effect to FGM2 is a clear indication that it is caused by the reconfigured OBDH which is located right below FGM2.

The next action was a redundancy switch of the PCDU causing only a short spike. Also the switch-over to Transmitter 2 and the related activation of the coax switch resulted only in a short spike. A small but clearly visible field change is related to the redundancy switch of the GPS receiver. Finally the ACC was switched to its redundant board. Concurrent with this change a huge magnetic spike occurred. It is generated by the electromagnetic proofmass exciter which is normally activated by telecommand but in this case triggered by the redundancy switch. Observed peak amplitudes are listed below. By determining the magnetic moment of the disturbance it is possible to predict the effect on the magnetometers in the deployed configuration. We obtain a magnetic moment with the components  $m_x = -800$ ,  $m_y = 800$ ,  $m_z = 0$  in  $\text{mAm}^2$ .

Table 7.1-2: Magnetic impulse generated by ACC exciter

Boom	FGM 1 [nT]			FGM2 [nT]		
	dX	dY	dZ	dX	dY	DZ
stowed	-266	-380	-583	106.4	-72.5	-106
deployed	-1.5	-0.7	0.1	-2.2	-1.1	0.3

Since the disturbance is very short-lived, just two samples in the FGM 50 Hz mode, it is of no concern for the measurement quality. On the other hand the FGMs can, however, be employed to verify the functioning of the exciter when it has been activated during the mission.

Redundancy Switching  
(boom stowed, 07.02.2000)

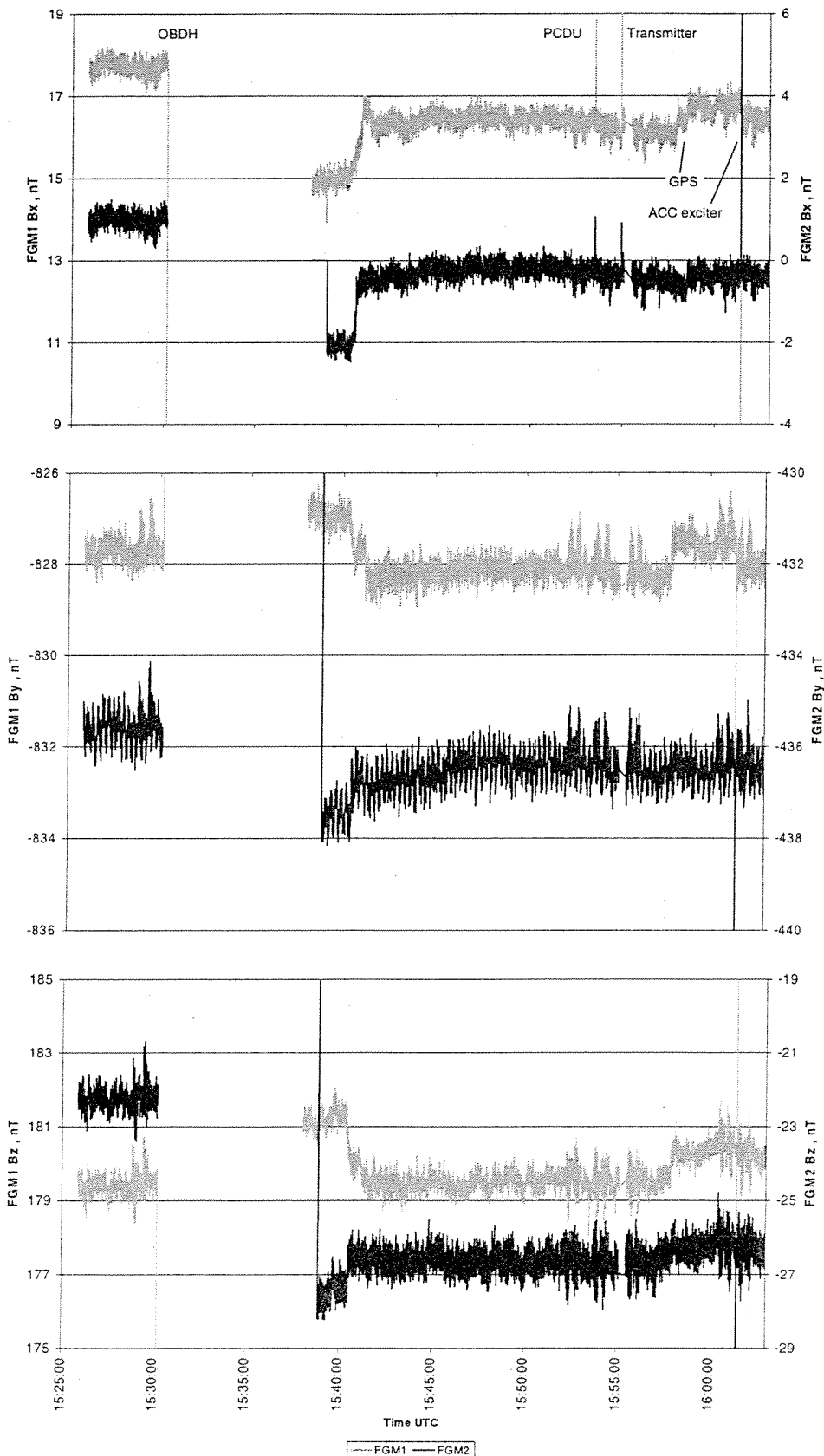


Figure 7.1-2 FGM 1 and 2 response to redundancy switching, boom stowed

## 7.2 Switching AOCS Components

In this section we present the observed magnetic effects caused by the AOCS components, except for the magnetorquers, which will be treated in a separate chapter (9). There are 14 cold gas thrusters on-board the CHAMP spacecraft. Figure 7.2-1 shows the magnetic deflections occurring when the individual thrusters are activated. Note that thruster 5 is disabled when the boom is stowed. In Table 7.2-1 the disturbances at the two FGMs are listed.

*Table 7.2-1: Deflections caused by the thrusters, boom stowed*

Thruster No	FGM 1 [nT]			FGM2 [nT]		
	dX	dY	dZ	dX	dY	dZ
T1	-3.7	-8.2	3.3	-3.7	-3.0	0
T2	4.3	-8.8	-2.4	4.0	-3.2	0
T3	4.3	9.2	-2.4	4.0	3.2	0
T4	-3.7	8.6	3.3	-3.7	3.2	0
T6	-1.4	0	0	-0.6	0	0
T7	11.7	0	1.7	24.2	0	39.7
T8	0	0	1.2	0	0	0
T9	-0.6	-1.2	0	0	0	0
T10	2.6	2.5	0	10.6	4.8	6.7
T11	-0.9	1.2	0	0	0	0
T12	2.9	-2.4	0	11.0	4.6	6.9
O1	-2.6	0	0	-1.1	0	0
O2	-2.6	0	0	-1.1	0	0

**Thruster Activation**  
(boom stowed)

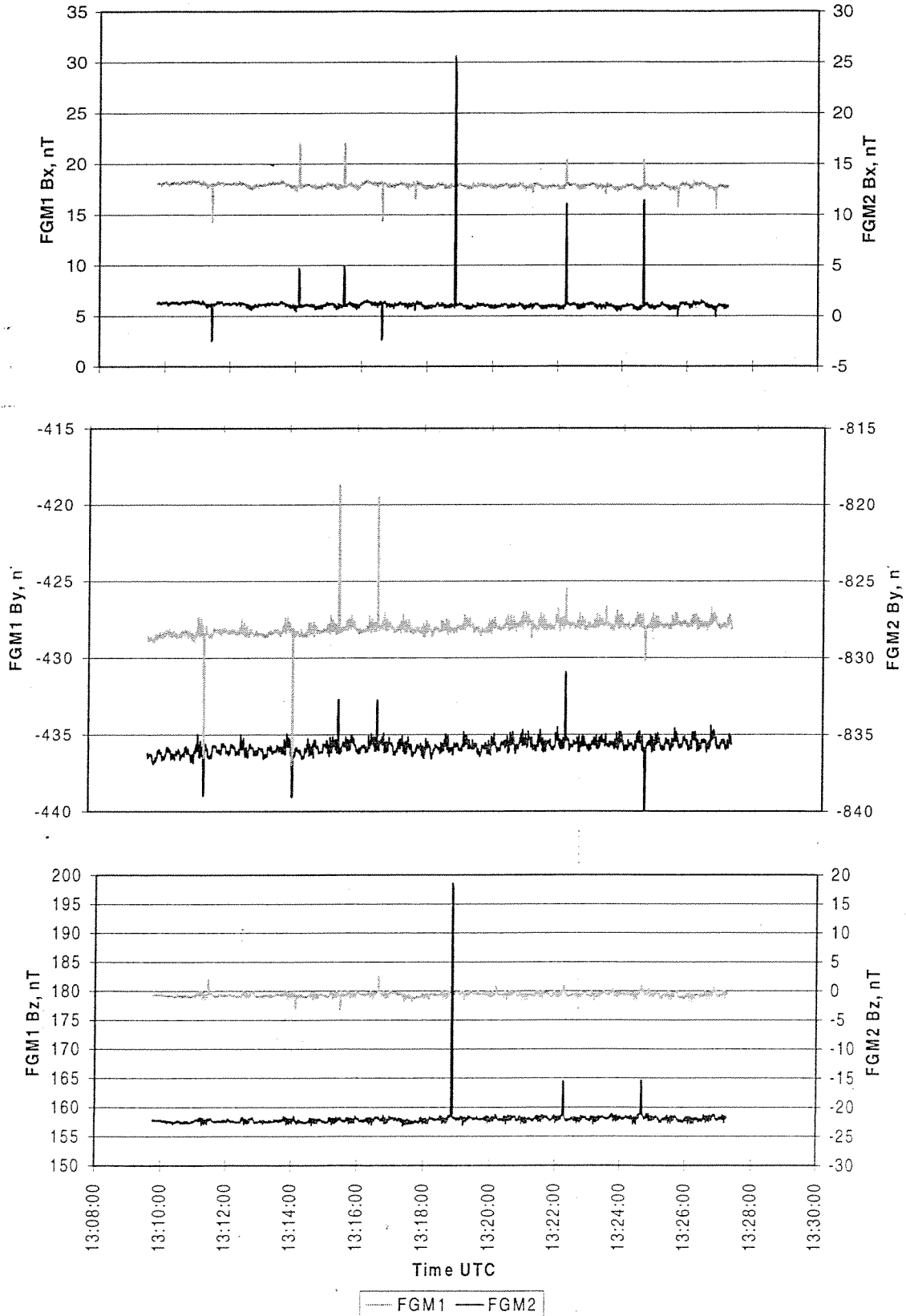


Figure 7.2-1 Magnetic disturbances caused by the thrusters, boom stowed



The magnetic effects of further AOCS components are shown in Figure 7.2-2. The initial small step in the curve is caused by the switch-on of the payload instruments. The subsequent prominent spike in the FGM1 recordings coincides with the switch of the AOCS actuators to ground control. Subsequently we find the magnetic response to closing the latch valve LV1. It causes a clear shift of the spacecraft field in the X and Z components. Closing also LV2 almost compensates the previous effect. After opening LV1 and 2 again the pyro lines 1 and 2 were armed causing short spikes in the FGM1 X and Z components. Since the pyros are only used for boom deployment, the spikes are of no concern.

*Table 7.2-2: Magnetic effects of closing the latch valves LV1 and LV2, boom stowed*

	FGM 1 [nT]			FGM2 [nT]		
	dX	dY	dZ	dX	dY	dZ
LV1	22.4	1	20.0	4.4	0.3	7.8
LV2	-23.6	-1	-21.0	-4.6	-0.3	-8.2

Knowing the position of the AOCS components we can estimate from the FGM readings the moments of the magnetic disturbances caused by these devices. For all the thrusters we obtain  $m = 120 \pm 10 \text{ mAm}^2$ . The orientation of the magnetic moment is in all cases anti-parallel to the thrust direction. For the latch valves we obtain a magnetic moment  $m = 495 \text{ mAm}^2$  (LV1) and  $m = 520 \text{ mAm}^2$  (LV2). With this information at hand we can predict the level of disturbance from any of these devices at the magnetometers in the deployed configuration. Table 7.2-3 lists field values in pT for FGM1 and FGM2.

*Table 7.2-3: Expected disturbances from AOCS components in deployed configuration*

Device	Dipole	FGM1 [pT]			FGM2 [pT]		
		dX	dY	dZ	dX	dY	dZ
T1	-mz	44	-8	97	74	-14	139
T2	+mz	-37	6	-101	-63	12	-145
T3	+mz	-3.7	-6	-101	-63	-12	-145
T4	-mz	44	8	97	74	14	139
T5	+mz	59	0	-675	126	0	-1479
T6	-mz	12	0	47	20	0	63
T7	-mz	115	0	243	243	0	400
T8	+mz	2	0	-44	3	0	-59
T9	+my	11	-44	0	17	-59	-1
T10	-my	194	392	-18	451	713	-56
T11	-my	11	44	0	17	59	-1
T12	+my	194	-392	-18	451	-713	-56
O1	+mx	91	-5	-6	121	-7	-9
O2	+mx	91	5	-6	121	7	-9

Device	Dipole	FGM1 [pT]			FGM2 [pT]		
		dX	dY	dZ	dX	dY	dZ
LV1	+mz	-25	1	-287	-45	1	-404
LV2	-mz	27	1	302	47	1	424

Considering the resolution of the FGMs (100 pT) only the action of a few of the thrusters will be visible. For FGM1 these are T5, T7, T10 and T12. When taking into account that in nominal operation always successive thrusters (T1+T2, T3+T4, etc.) are fired simultaneously we obtain a good self-compensation for rotations about the S/C x axis (T1 – T4), but we are left with noticeable disturbances for maneuvers about the other two axes.

Closing one of the latch valves will shift the spacecraft static field by a few tenths of a nano Tesla. Fortunately, the major part of this effect will be corrected with the help of the OVM-FGM cross-calibration. However, switching a latch valve will considerably change the S/C magnetic moment and may affect the attitude control.

**Latch Valves**  
(boom stowed)

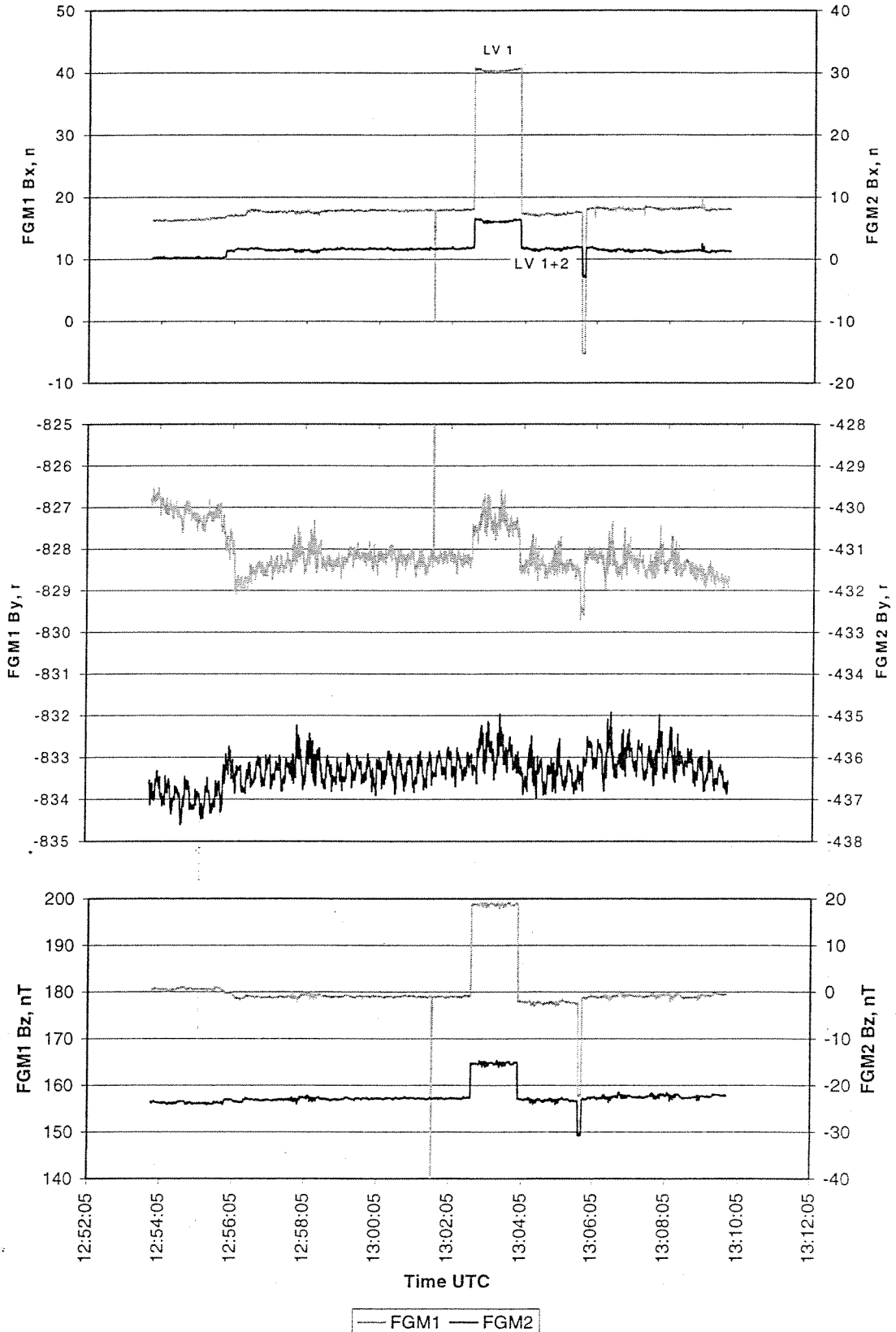


Figure 7.2-2 Magnetic effect of the AOCs components, boom stowed

### 7.3 Switching the Heaters

For maintaining a suitable thermal environment the CHAMP spacecraft is equipped with 22 electrical heaters. These have been switched on successively to determine their magnetic effect. Figure 7.3-1 shows the increase of combined heater current when activating more and more heaters. Finally we reach a peak current of 3.9 A. Subsequently all heaters were switched off at once.

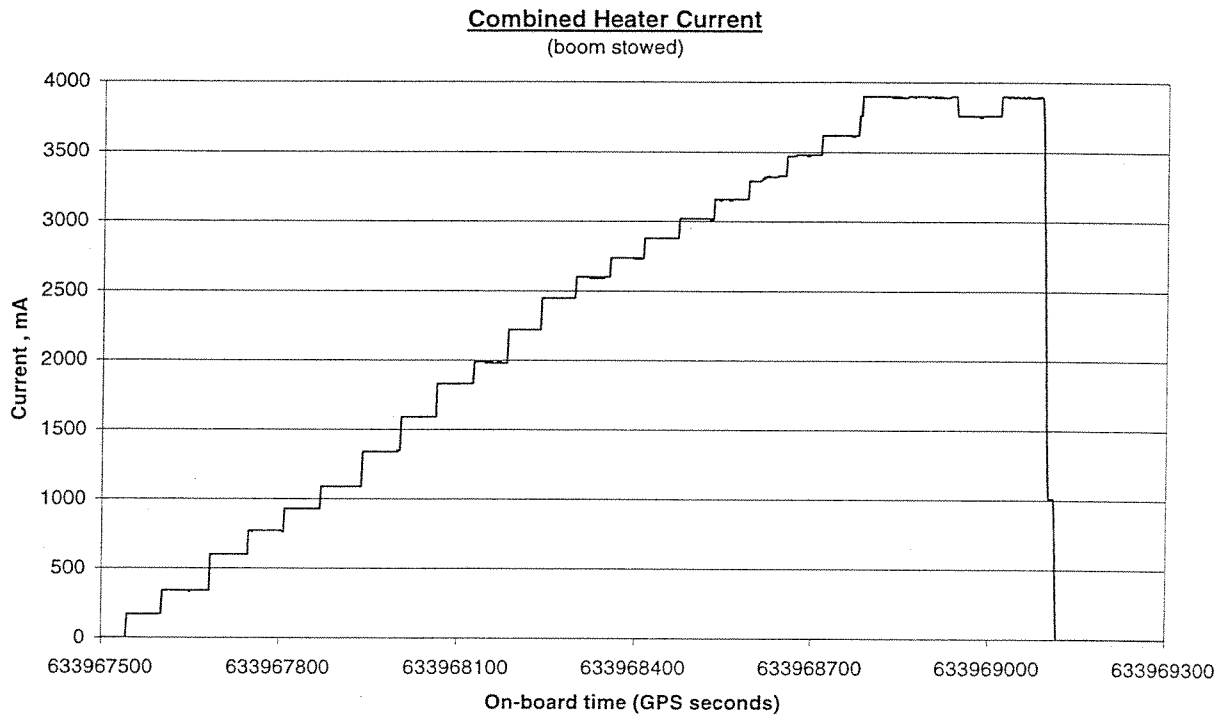



Figure 7.3-1 Combined heater current

The corresponding magnetic field recordings are shown in Figure 7.3-2. We see a gradual but continuous change in all components and a clear jump back when the heaters are switched off. The lack of heater-related signatures in the magnetic recordings strongly suggests that the heaters themselves cause no magnetic disturbances. The gradual change in the field components probably reflects the general increase in bus power. From the final step-like change related to heater switch-off we read the following deflections.

Table 7.3-1: Magnetic effect when all heaters are switched on, boom stowed

FGM 1 [nT]			FGM2 [nT]		
DX	dY	dZ	dX	dY	dZ
1.8	1.5	-1.3	0.9	0.7	-0.6

Here we can again make use of the dual magnetometer technique to spot the disturbance dipole. Our estimate reveals a location in the battery compartment. For a current draw of 3.9 A

	<b>CHAMP Magnetic Test Report</b>	Doc: CH-GFZ-TR-2000 Issue: 1.0 Date: 15.06.2000 Page: 29 of 51
---	---------------------------------------	---

a magnetic moment of about 110 mAm<sup>2</sup> ( $m_x = 65$ ,  $m_y = 85$ ,  $m_z = 0$ ) emerges. Since the installed battery was not under power, the disturbances probably emanated from the supply umbilical.

In summary, we may state that none of the bus and payload units generates excessive magnetic disturbances. This is furthermore a good indication that the single point grounding concept has consequently been realized throughout the whole system and also other rules for reducing magnetic stray field have been obeyed .

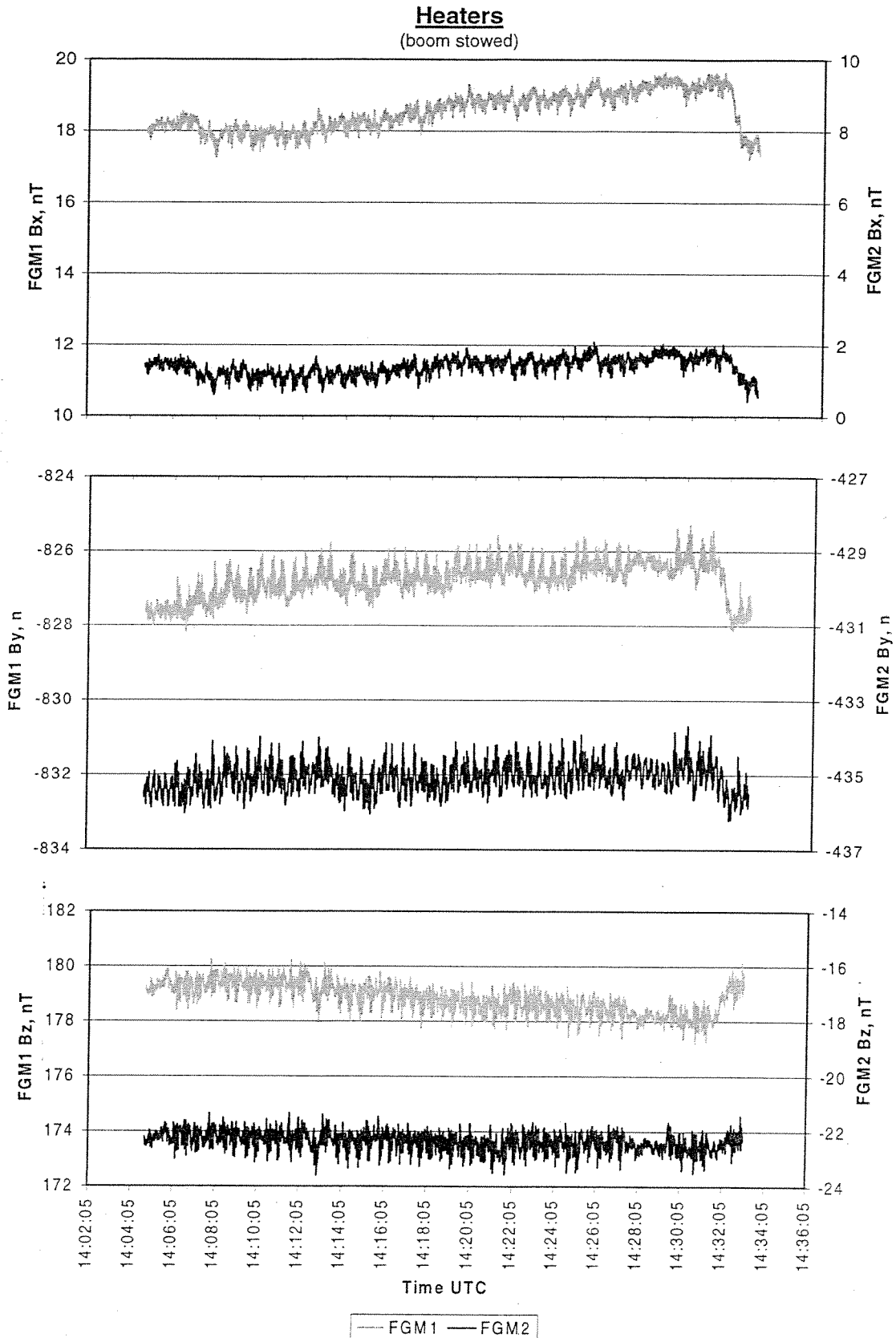



Figure 7.3-2 Magnetic effect of heater current, boom stowed

	<b>CHAMP Magnetic Test Report</b>	Doc: CH-GFZ-TR-2000 Issue: 1.0 Date: 15.06.2000 Page: 31 of 51
---	---------------------------------------	---

## 8 STRAY FIELD, BOOM DEPLOYMENT

The test sequence described in the previous chapter was almost completely repeated, but in the deployed boom configuration which is the nominal in-orbit configuration. Great care was taken to orient the spacecraft parallel to the facility axes. Also the deployment angle of the boom,  $1.82^\circ$  below horizontal, was adjusted as good as possible. The chosen test set-up is depicted in Figure 4.1-4. During this test the spacecraft was placed at reference point RP3 which means that FGM was in the center of the facility. No measurements have been performed with the facility Förster magnetometers. To allow for a proper operation of the OVM a constant field of 50000 nT was applied by the facility in the North direction.

### 8.1 Switch-on of Instruments

According to the results from the previous chapter only a few disturbances should be visible in this configuration. In fact there is only one significant response in Figure 8.2-1, showing the payload switch-on sequence, which is related to the power-up of the ASC-A. The cause for this deflection was already discussed in Section 7.1. The observed deflections at FGM2 are:  $dx = 0.4$  nT,  $dy = 0.3$  nT and  $dz = 0.4$  nT. During this test the baffle apertures were closed by black card-board to avoid over-exposure. This action resulted in a clear reduction of the disturbance level (cf. Table 7.1-1).

A similar result is obtained with the redundant components. Here we find, as expected, only the short spike caused by the proofmass exciter of the STAR accelerometer when it is switched to its redundant board. The observed peak deflections are at FGM1:  $dx = -1.2$ ,  $dy = -0.5$ ,  $dz = 0.3$  nT and at FGM2:  $dx = -2.1$ ,  $dy = -0.9$ ,  $dz = 0.4$  nT (cf. Table 7.1-2).

### 8.2 Switching AOCs Component

This part of the test provides us with a good opportunity to verify the predicted magnetic disturbances of the thrusters at the locations of the FGMs. As can be seen in Figure 8.2-2 pulses sticking out of the noise at FGM2 are related to the activation of T5 ( $B_z$ ), T10 ( $B_y$ ), T12 ( $B_x$ ,  $B_y$ ). The observed deflections fit well the predicted amplitudes (cf. Table 7.2-3) which confirms the validity of magnetic moment estimates. Closing the latch valves LV1 and LV2 causes a deflection of about 0.5 nT and  $-0.5$  nT, respectively, in the FGM2  $B_z$  component. This is again consistent with the prediction.

As expected there is no influence of the heaters observed at the magnetometers.

Instrument Switch-On  
(boom deployed)

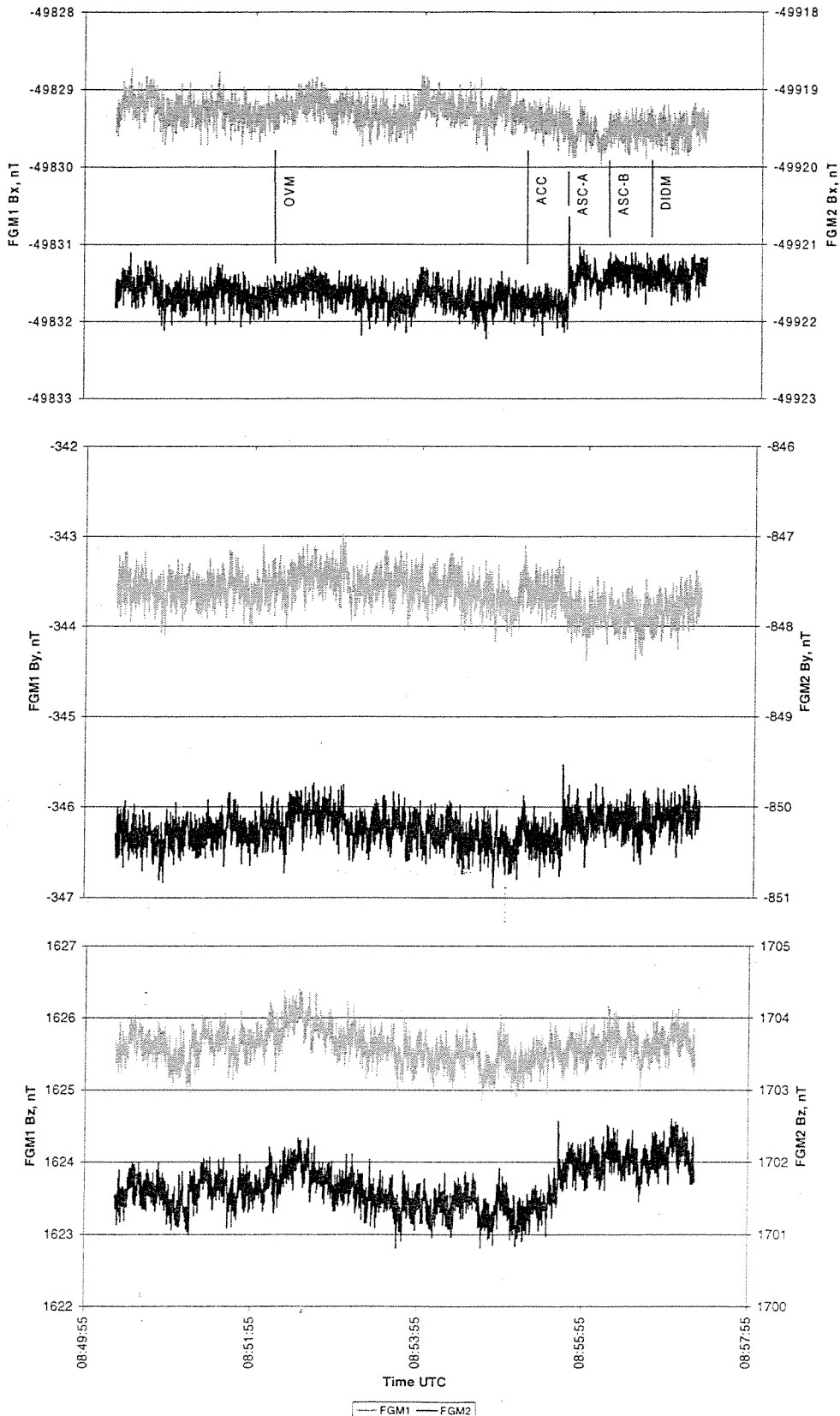


Figure 8.2-1 FGM 1 and 2 response to instrument switch-on, boom deployed



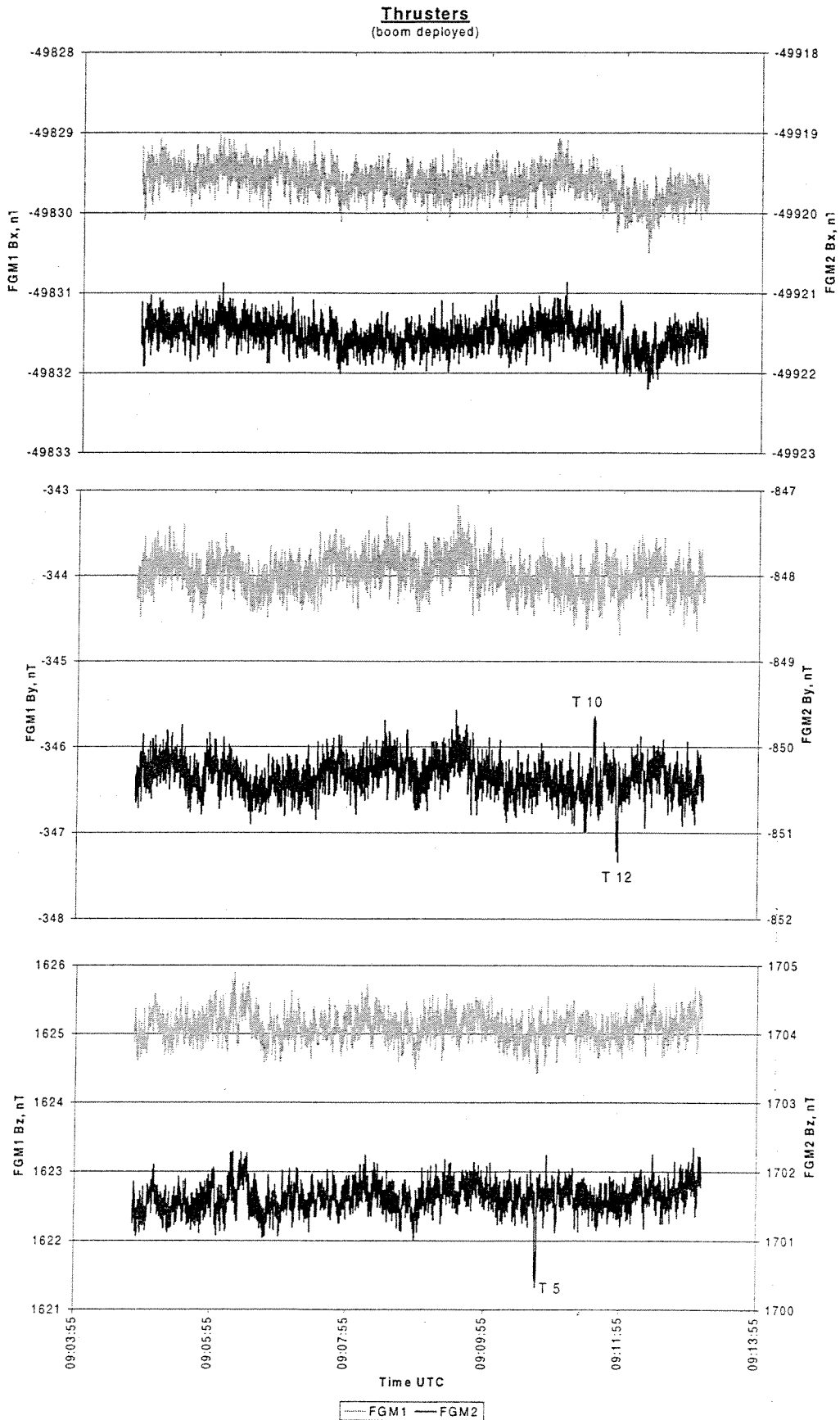


Figure 8.2-2 Magnetic disturbance caused by the thrusters, boom deployed

## 9 PROPERTIES OF THE MAGNETORQUERS

The CHAMP spacecraft has magnetorquers which are intended to support the cold gas attitude control system. There are redundant coils for each of the three principal axis. The torquers are designed to generate a magnetic moment of 6.4 Am<sup>2</sup> when supplied with a current of 314 mA. The generated magnetic field causes a significant deflection at the on-board magnetometers. It is thus important to perform a proper calibration of the torquers influence. Otherwise it would not be possible to correct effectively for this disturbance. In the subsequent sections we will present the results for a stowed and deployed boom configuration. The obtained numbers will be used in the magnetometer data processing software.

### 9.1 Stowed Boom Configuration

Nominally it is not foreseen to operate the torquers as long as the boom is stowed. From the operational point of view there are, however, no restrictions which would not allow it. For completeness we thus performed a full calibration sequence also in this configuration. The current through the torquer coils was varied over the whole range from 300 mA to -300 mA. Magnetic field readings were taken at steps of 100 mA. A linear regression was applied for determining the response function. For the compensation of the torquer effects on the magnetic field measurements, the applied currents have to be multiplied with the torquer correction matrix T.

$$\begin{pmatrix} b_{TX} \\ b_{TY} \\ b_{TZ} \end{pmatrix} = \begin{pmatrix} T \\ \\ \end{pmatrix} \cdot \begin{pmatrix} I_X \\ I_Y \\ I_Z \end{pmatrix} \quad (9.1-1)$$

where  $I_X$ ,  $I_Y$ ,  $I_Z$  are the applied torquer currents in Ampere and  $b_{TX}$ ,  $b_{TY}$ ,  $b_{TZ}$  are the resulting magnetic deflections in nT. These deflections have to be subtracted from the magnetometer readings.

$$\begin{aligned} B_X &= B_{FGMX} - b_{TX} \\ B_Y &= B_{FGMY} - b_{TY} \\ B_Z &= B_{FGMZ} - b_{TZ} \end{aligned} \quad (9.1-2)$$

Below the elements of the torquer correction matrices are listed.

Table 9.1-1: Elements of the torquer correction matrices (boom stowed)

FGM1 :	Main			Redundant		
	1	2	3	1	2	3
Element						
1	-458	-1739	-3290	-444	-1706	-3400
2	-5	-287	-17	-5	-125	-18
3	171	-3827	-627	164	-3736	-549

FGM2 : Element	Main			Redundant		
	1	2	3	1	2	3
1	-218	1589	-3379	-213	1587	-3764
2	-5	-242	-29	-5	-75	-31
3	64	-4174	-11601	61	-4089	-12501

The numbers listed in Table 9.1-1 reflect the magnetic effect in nT per Ampere current through the torquer coils. Particularly large deflections at FGM2 are caused by the Z torquer (last column). It is also surprising to see that the Y torquer (middle column) generates the smallest effect in the Y components at both FGMs. The reason for this is the soft magnetic forward cold gas tank which causes a significant distortion of the torquer field.

During the test it was speculated whether the nearby Y torquer would modify the magnetic properties of the tanks. To check that, the Y torquer was operated through a full cycle from zero up to 300 mA then down to -300 mA and back to zero. Our aim was to look for hysteresis effects. Fortunately, no such effect was found.

Furthermore, initiated by the above observations the question came up how the forward cold gas tank modifies the overall performance of the Y torquer. To answer this question a dedicated test of the torquer field distribution was performed. A series of magnetometers (FM1 through FM4) was installed along the coil axis at distances of 1.1, 1.6, 2.1 and 2.6 m from the torquer. Measurements were taken on both sides of the spacecraft. Field strengths observed at the four positions caused by a 600 mA current step are listed below.

*Table 9.1-2: On-axis field distribution of the Y torquer*

	FM1: 1.1 m	FM2: 1.6 m	FM3: 2.1 m	FM4: 2.6 m
Starboard	1526 nT	524 nT	239 nT	127 nT
Port	1797 nT	537 nT	243 nT	129 nT

After adjusting the effective distances by some 2 cm a good agreement with a dipole decay is reached for all measurements except for those at 1.1 m. For the attitude control the near-field distribution is of no concern. The resulting dipole moment for a 300 mA current is 5.7 Am<sup>2</sup>. All this means that there are no significant influences of the soft magnetic tanks on the torquer efficiency to be expected.

## 9.2 Deployed Boom Configuration

During nominal operation in particular in the Fine Pointing Mode all three torquers are continuously in operation. Even with the boom deployed they have a significant influence on the magnetic field measurements. In order not to spoil the highly accurate magnetic field measurements, a dedicated calibration of the torquer influence was performed. In a first run the currents applied to the torquer coils were varied in steps of 50 mA from 300 mA to -300 mA and readings were taken at each step with all three magnetometers. A linear regression between the applied currents and the recorded magnetic deflections revealed again consistent results with residuals ranging around 0.1 nT. Below the elements of the torquer correction matrix resulting from the correlation analysis are listed.

Table 9.2-1: Elements of the torquer correction matrix (boom deployed)

FGM1 : Element	Main			Redundant		
	1	2	3	1	2	3
1	15.2	-9.2	-14.3	15.1	-9.7	-13.6
2	-0.3	-27.0	-0.3	0.3	-26.7	0.1
3	-1.3	1.5	-35.9	-1.3	1.3	-36.0

FGM2 : Element	Main			Redundant		
	1	2	3	1	2	3
1	20.4	-16.7	-28.9	20.3	-17.5	-27.8
2	-0.5	-42.7	-1.0	0.5	-42.3	-0.6
3	-1.9	3.2	-59.0	-2.0	3.0	-59.3

The magnetic field correction procedure is the same as outlined in the previous section (Equation (9.1-1)).

Not only the FGMs but also the OVM is affected by the torquers. The determination of the disturbances is not as straight forward. Since we are dealing with a scalar magnetometer, only the part of the field aligned with the background field will have an effect. Therefore dedicated field settings were required for the determination of the complete matrix. The elements of the applicable correction matrix are listed below.


Table 9.2-2: Torquer correction matrices for OVM

OVM : Element	Main			Redundant		
	1	2	3	1	2	3
1	7.3	-2.6	-2.7	7.2	-2.65	-2.44
2	0	-9.8	0	0	-9.7	0
3	-0.6	0.5	-11.6	-0.6	0.5	-11.6

For the correction of the torquer effect first the deflection at the position of the OVM has to be calculated according to equation (9.1-1). In a subsequent step the OVM readings are corrected as shown.

$$B = B_{OVM} - (Xb_{TX} + Yb_{TY} + Zb_{TZ}) / B_{OVM} \quad (9.2-1)$$

where X, Y, Z are the magnetic field components in spacecraft coordinates, as determined by FGM.

	<b>CHAMP Magnetic Test Report</b>	Doc: CH-GFZ-TR-2000 Issue: 1.0 Date: 15.06.2000 Page: 37 of 51
---	---------------------------------------	---

### 9.3 Timing of the Torquer Control

During the mission the torquer settings will be changed every second. For that reason it is not sufficient to know the scale value of the correction, but it is also important to know the time of field change and to take the response of the instruments to a step-like field change into account.

The dynamic response of the magnetometers has been determined in previous tests (OVM: [RD 07] and FGM: [RD 03]). According to the spacecraft manufacturer, the actual current through the torquers which is affiliated with a time stamp  $t_0$  has been applied at  $t_0-95$  ms. Depending on the sample rate the calculation of the effective current  $I_T$  for equation (9.1-1) has to be done as follows:

FGM (50 Hz)

$$I_T(t_s) = I_T(t_{-1}) \quad \text{for } t_0 - t_s \leq 0.885 \quad (9.3-1)$$

$$I_T(t_s) = \frac{t_s - t_{-1} - 0.885}{0.04} [I_T(t_0) - I_T(t_{-1})] + I_T(t_{-1}) \quad \text{for } 0.885 < t_0 - t_s < 0.925$$

$$I_T(t_s) = I_T(t_0) \quad \text{for } t_0 - t_s \geq 0.925$$

where  $t_s$  is the FGM sample time in sec.

FGM (10 Hz)

$$I_T(t_s) = I_T(t_{-1}) \quad \text{for } t_0 - t_s \leq 0.855 \quad (9.3-2)$$

$$I_T(t_s) = \frac{t_s - t_{-1} - 0.855}{0.1} [I_T(t_0) - I_T(t_{-1})] + I_T(t_{-1}) \quad \text{for } 0.855 < t_0 - t_s \leq 0.955$$

$$I_T(t_s) = I_T(t_0) \quad \text{for } t_0 - t_s \geq 0.955$$

This last interval is probably of no relevance, since it is void of any reading in the 10 Hz mode.

FGM (1 Hz)

$$I_T(t_s) = (t_s - t_{-1} - 0.505) \cdot [I_T(t_0) - I_T(t_{-1})] + I_T(t_{-1}) \quad (9.3-3)$$

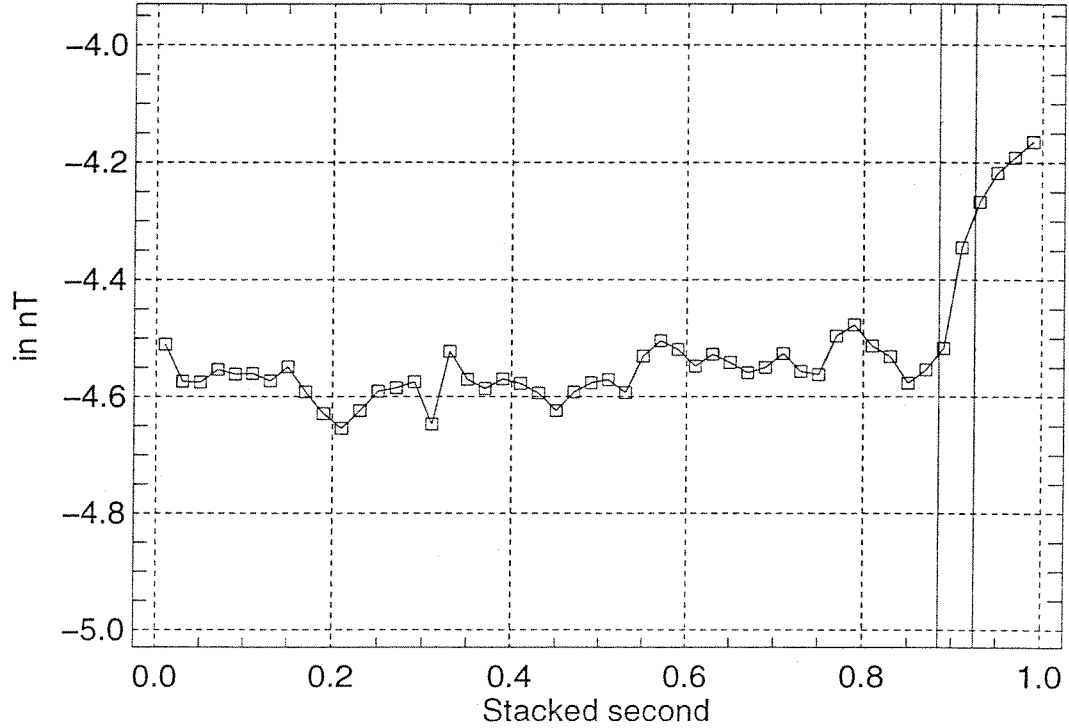
A similar relation holds for the OVM

$$I_T(t_s) = 0.25I_T(t_{-2}) + 0.75I_T(t_{-1}) \quad (9.3-4)$$

where the times  $t_1$  and  $t_2$  correspond to data packages 1 and 2 sec before the actual, one ( $t_0$ ) respectively.

The above mentioned time for updating the torquer currents has been confirmed during this test. As an example the magnetic effect of the torquer on the FGM 1 and 2 z-component is shown in Figure 9.3-2 and 9.3-2 respectively.

FGM 1, AOCS, Z, no trq-corr,  
stacked seconds, 40:60 sec, GPS offset =641027746



FGM 1, AOCS, Z, corrected,  
stacked seconds, 40:60 sec, GPS offset =641027746

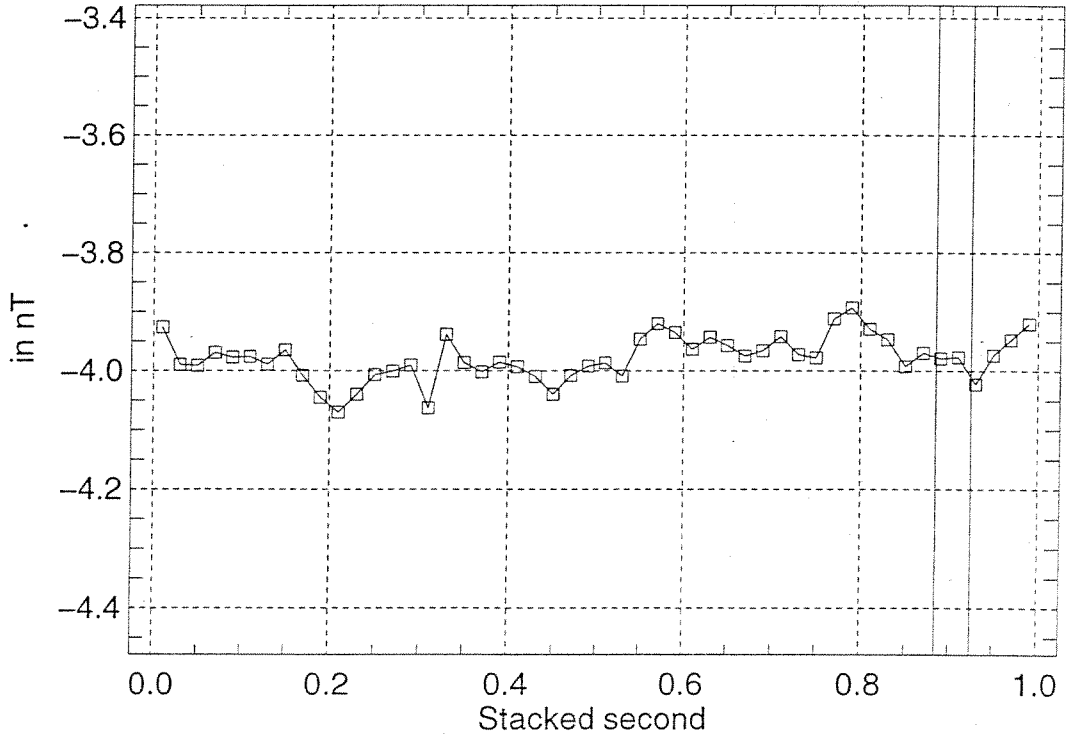
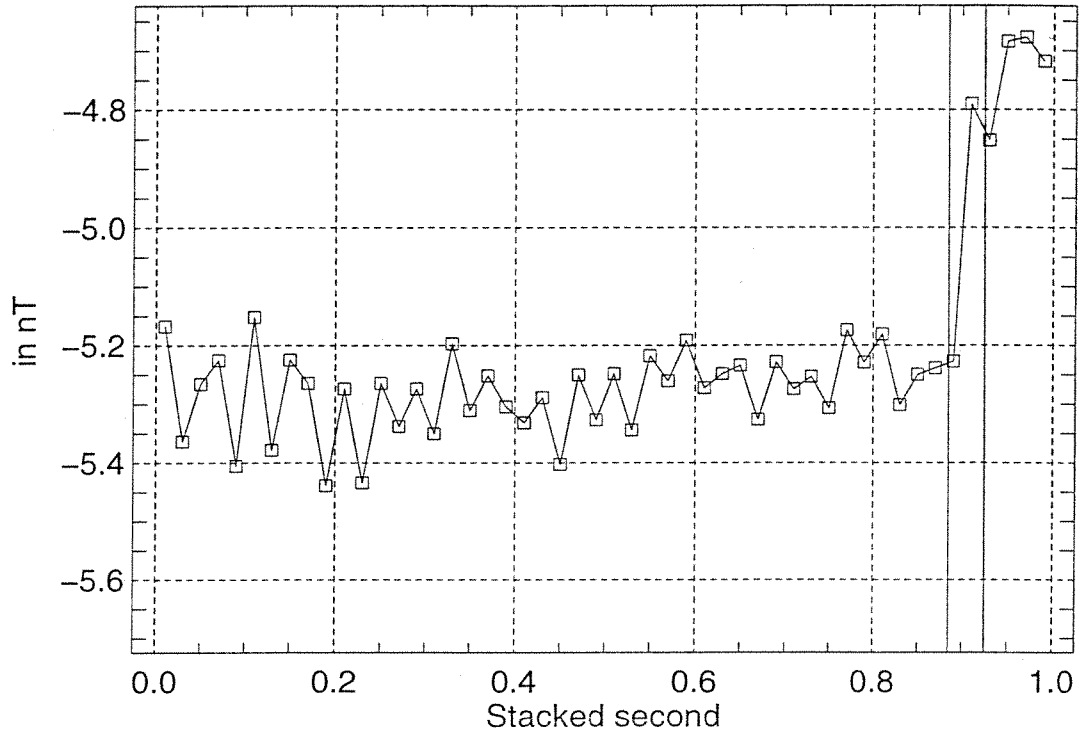


Figure 9.3-1 FGM1 recording: (top) without , (bottom) with torquer correction

FGM 2, AOCS, Z, no trq-corr,  
stacked seconds, 40:60 sec, GPS offset =641027746



FGM 2, AOCS, Z, corrected,  
stacked seconds, 40:60 sec, GPS offset =641027746

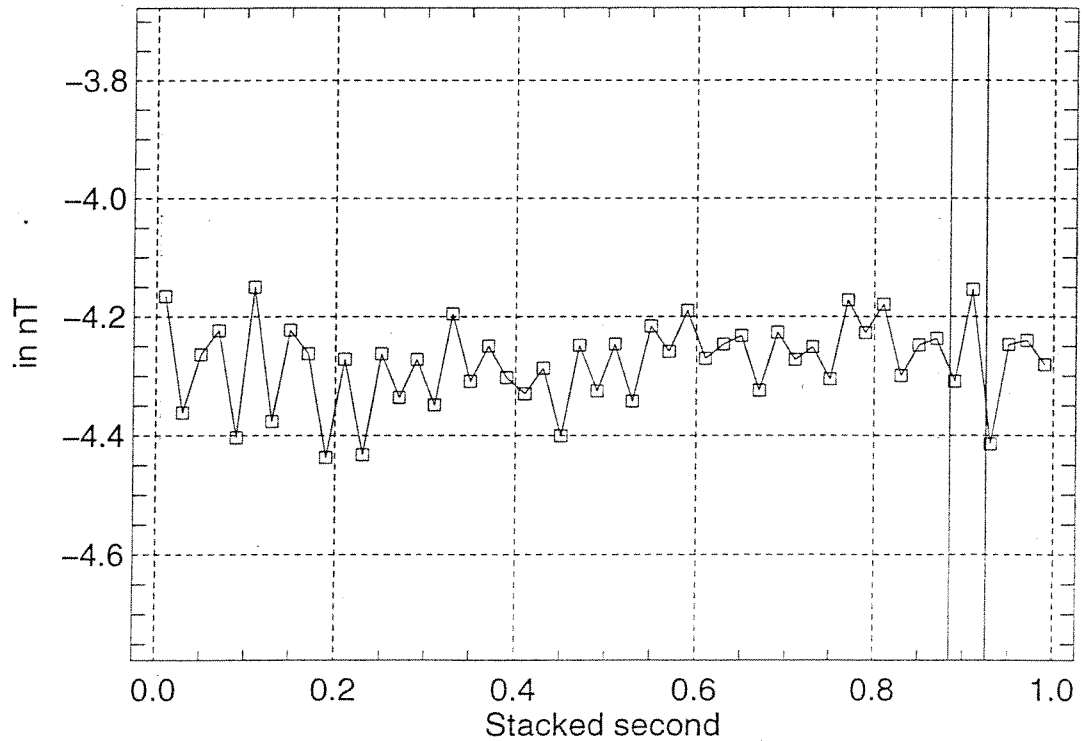



Figure 9.3-2 FGM2 recording: (top) without , (bottom) with torquer correction

	<b>CHAMP Magnetic Test Report</b>	Doc: CH-GFZ-TR-2000 Issue: 1.0 Date: 15.06.2000 Page: 40 of 51
---	---------------------------------------	---

## 9.4 Performance of the Torquers

The magnetic test also allows to determine the performance of the torquers on system level. We have used the FGM1 readings to estimate the magnetic moments. The underlying formula for the dipole moment  $M_m$  is:

$$M_m = \frac{Br^3}{100\sqrt{1+3\cos^2\theta}} \quad (9.4-1)$$

where B is the field magnitude in nT, r the separation distance in m and  $\theta$  the angle between the dipole axis and line connecting the dipole and the magnetometer. For the moments we obtained when applying a 300 mA current:

$$M_x = 5.81 \text{ Am}^2, \quad M_y = 5.88 \text{ Am}^2 \quad \text{and} \quad M_z = 5.84 \text{ Am}^2$$

This is about 4% less than the designed moments.

There is no appreciable difference obtained for the redundant torquers.

## 10 ORIENTATION OF THE FGMs

There are a number of applications where the magnetic field vector in S/C coordinates is required (e.g. attitude control, Lorentz force correction, electric field estimate, etc.). Since the FGMs are employed to determine the field components, the orientation of their magnetic axes with respect to the S/C frame has to be known. The level of required precision is quite different for the various applications, we therefore present two independent sets of transformation matrices.

### 10.1 FGM Transformation Matrices for AOCS

The Attitude and Orbit Control System (AOCS) needs to know the orientation of the ambient magnetic field vector wrt. the S/C coordinates to be able to make effective use of the magnetorquers for attitude control. In the case of CHAMP raw data of the FGMs are routed directly to the AOCS. The magnetic field range of  $\pm 65 \mu\text{T}$  is covered by a 16 bit word with a quantization step size of 2 nT.

Transformation matrices are needed for both the stowed and deployed boom configuration. The quality of the magnetic field data in the stowed configuration is clearly reduced due to the proximity to magnetic disturbers. Angular uncertainties up to  $1^\circ$  are expected. For this reason the matrix does not need to be very detailed. The transformation is done as follows

$$B_{S/C} = A \cdot B_{FGM} \quad (10.1-1)$$

In the stowed boom configuration the transformation matrix A is identical for the FGM1 and FGM2



$$A = \begin{pmatrix} -1 & 0 & 0 \\ 0 & 1 & 0 \\ 0 & 0 & -1 \end{pmatrix}$$

In the deployed configuration which is foreseen during nominal operation, it is worth taking more details into consideration.

*Table 10.1-1: Elements of FGM transformation matrices, boom deployed*

Element	FGM1			FGM2		
	1	2	3	1	2	3
1	1.002	0.0071	-0.0328	1.000	0.0168	-0.0335
2	-0.0071	1.002	0.0057	-0.0168	1.004	-0.001
3	0.0328	-0.0057	1.002	0.0335	0.001	1.001

The determinants of these matrices differ from unity, because they are not just pure rotation matrices. The sensor data have not been orthonormalized before transmission.

## 10.2 FGM Transformation Matrices for Science Application

All the data used in scientific applications are derived from the high resolution science data stream, and they go through a post-processing removing all instrumental effects before they are transformed into the dedicated coordinate system. Some of the pre-processing steps are outlined in the next chapter.

Although scientific measurements are not foreseen in the stowed configuration we give here for completeness also the matrices which transform the FGM measurements into the S/C system.

*Table 10.2-1: Elements of the matrices for transforming FGM data into the S/C system (boom stowed)*

Element	FGM1			FGM2		
	1	2	3	1	2	3
1	-0.999979	0.001050	0.006356	-0.999964	-0.008443	-0.001017
2	0.00086	0.999984	0.005592	-0.008441	0.999964	-0.000804
3	-0.00635	0.005599	-0.999964	0.001025	-0.000795	-0.999999

Euler angles 1-2-3, FGM1:  $\phi = 0.3208^\circ$ ,  $\theta = 180.3638^\circ$ ,  $\psi = 0.0622^\circ$

FGM2:  $\phi = -0.0456^\circ$ ,  $\theta = 179.9413^\circ$ ,  $\psi = -0.4837^\circ$

These matrices reflect misalignment angles of less than  $0.5^\circ$ .

Much more important is the relative attitude of the FGMs with respect to the S/C coordinate system when the boom is deployed. We decided to have a common transfer matrix for the two magnetometers.

This common magnetometer frame is based on the orthogonalized coil axes of the FGM1. The last step in pre-processing the FGM2 data is therefore a transformation into the FGM1 frame.

*Table 10.2-2: Matrix for transforming FGM2 into FGM1*

Element	1	2	3
1	0.999959	0.009012	-0.000913
2	-0.009018	0.999935	-0.006970
3	0.00085	0.006978	0.999975

This matrix is equivalent to three consecutive Euler rotation about the axes X, Y, Z. The associated angles are:

$$\phi = -0.398^\circ \quad \theta = 0.0487 \quad \psi = 0.5167$$

Compared to previous measurements in Autumn 1998 [RD 03] these angles have changed only by some 10 arcsec. They can be determined in orbit and will be used as an indicator for the stability of the optical bench.

The final transformation from the FGM1 frame to the S/C system is strongly dependent on the actual orientation of the deployed boom with respect to the spacecraft. We tried to adjust the deployment angle during the magnetic field test as good as possible, but uncertainties of the order of  $0.1^\circ$  compared to the flight configuration are expected. The obtained transformation should thus be considered as initial value.

*Table 10.2-3: Matrix for transforming FGM1 into the S/C system*

Element	1	2	3
1	0.999417	0.006987	-0.033404
2	-0.006808	0.999962	0.005467
3	0.033441	-0.005237	0.999427

Associated Euler angles for a 1-2-3 rotation are:

$$\phi = 0.3002^\circ \quad \theta = 1.9164^\circ \quad \psi = 0.3903^\circ$$

In case of a significant difference in deployment angle  $\theta$  also the determined torquer correction functions are questionable. Deviations by more than  $0.2^\circ$  will require a new calibration of the torquer effects.

## 11 CHARACTERISTICS OF THE MAGNETOMETERS

The magnetic system test gave us the chance to verify the performance of the magnetometers in the fully integrated configuration. There are a few limitations which have to be considered when interpreting the test data. The largest problems are caused by the field gradients in the coil facility. The size of the homogeneous volume is not large enough to allow for a direct comparison between the readings of the OVM and the FGMs with full precision. To overcome this problem independent measurements with either the OVM or FGM 1 in the center of the facility were performed.

### 11.1 Non-Linearity Coefficients of the FGMs

If one wants to make full use of the high precision provided by the FGMs a slight non-linearity of the analog-to-digital converters (ADC) has to be taken into account. The ADCs have been tested in the laboratory on component level for their non-linear characteristics, but there has never been a verification on system level.

For this test the spacecraft was positioned at reference point RP3. Magnetic fields were applied by the coil facility. Starting with 63  $\mu\text{T}$  the field was reduced in steps of 3  $\mu\text{T}$  until 18  $\mu\text{T}$  was reached. This is the lower limit of the OVM range. Then we switched to -18  $\mu\text{T}$  and continued in steps of 3  $\mu\text{T}$  down to -63  $\mu\text{T}$ . The same procedure was performed for the X, the Y and the Z component. All three magnetometers were operated simultaneously.

For the evaluation of the non-linearity first the field magnitude as determined by the three components of the fluxgates was computed. These numbers were compared to the OVM readings and a third order polynom was fitted to the relation. Judging from the residuals, a very good fit was achieved. They all range around 0.1 nT except for field values around 45  $\mu\text{T}$  where we have a known slight anomaly in the ADCs. The obtained non-linearity coefficients are listed below.

*Table 11.1-1: Non-linearity coefficients of FGMs*

	Second order terms in $10^{-10}$			Third order terms in $10^{-14}$		
	X	Y	Z	X	Y	Z
FGM1	8.242	7.952	6.838	1.98	1.85	1.79
FGM2	7.143	10.772	9.600	1.71	2.50	2.40

The reference readings were taken by the OVM about 2 m away from the FGMs. We argue that the inhomogeneity of the field in the facility does not influence the presented results. It is known that the scale factor and the offset are different at these two points, but it is hard to imagine that the non-linear coefficients are effected as long as there is no magnetic material between the magnetometers.

Comparing the achieved coefficients with previous calibrations we find that the second order terms all fall in between the lab results and the calibration in Autumn 1998 [RD 03]. The third order coefficients are all slightly smaller. All this shows that these coefficients were virtually constant over the last two years.

The FGM data have been corrected for the non-linearity with the coefficients derived here before calculating the instrument parameters presented in the subsequent section.

## 11.2 Calibration of the Coil Facility

Because of the high demands on accuracy in this test we first had to check the parameters of the coil facility. We employed the CHAMP OVM as the reference instrument. The spacecraft was moved to reference point RP4 which places the OVM sensor in the center of the facility. A thin shell run with 82 well distributed field directions and a constant magnitude of 50  $\mu\text{T}$  was applied. The parameters have been determined in an iterative fashion by comparing the field settings to the measured field magnitude.

*Table 11.2-1: Parameters of the coil facility*

Scale factors	$S_W = 1.000025 \text{ nT/EU}$
	$S_N = 0.9999384 \text{ nT/EU}$
	$S_D = 0.9999414 \text{ nT/EU}$
Offsets	$O_W = 6.03 \text{ nT}$
	$O_N = -28.97 \text{ nT}$
	$O_D = -4.50 \text{ nT}$
Misalignment angles	$(W,N) = 90.0015^\circ$
	$(W,D) = 90.0036^\circ$
	$(N,D) = 90.0007^\circ$

These values were obtained at a temperature of  $18.5^\circ \pm 0.3^\circ\text{C}$ . Because of the close control of the facility temperature, the parameters can be regarded as constant. These parameters have been used for the vector calibration of the FGMs.

## 11.3 Vector-Calibration of the FGMs

The FGMs have earlier been subjected to a number of dedicated tests to check their performance. Particularly intensive calibrations were performed in the magnetic facility of the IABG in Autumn 1998 [RD 03]. Although we are aware of the fact that the circumstances at this test are not ideal, we tried to retrieve the instrument parameters. Measurements were made in the boom stowed and deployed configuration. As usually, 82 field settings with random directions and a magnitude of 50  $\mu\text{T}$  were applied by the facility. In a first step the applied fields were corrected with the above listed parameters and then the FGM measurements have been compared to these settings. For the test with the stowed boom the spacecraft was located at reference point RP2.

*Table 11.3-1: Parameters of FGM1, boom stowed*

Scale factors in nT/EU (sensor temperature: 19°C)	CSC2 off	CSC2 on
	$S_x = 1.002907$	$S_x = 1.003128$
	$S_y = 1.007773$	$S_y = 1.007636$
	$S_z = 0.995121$	$S_z = 0.994978$
Offsets	$O_x = 40.2 \text{ nT}$	
	$O_y = -839.0 \text{ nT}$	
	$O_z = 174.1 \text{ nT}$	
Misalignment angles	$(X,Y) = 89.9684^\circ$	
	$(X,Z) = 89.5654^\circ$	
	$(Y,Z) = 89.9669^\circ$	

*Table 11.3-2: Parameters of FGM2, boom stowed*

Scale factors in nT/EU (sensor temperature: 19°C)	CSC1 off	CSC1 on
	$S_x = 0.999185$	$S_x = 0.999406$
	$S_y = 1.006672$	$S_y = 1.006535$
	$S_z = 0.997980$	$S_z = 0.997836$
Offsets	$O_x = 22.9 \text{ nT}$	
	$O_y = -444.0 \text{ nT}$	
	$O_z = -31.8 \text{ nT}$	
Misalignment angles	$(X,Y) = 89.9298^\circ$	
	$(X,Z) = 90.3945^\circ$	
	$(Y,Z) = 89.9212^\circ$	

It is not foreseen to use the magnetic field readings for scientific purposes in the stowed configuration, but for completeness these numbers are listed here. Because of the proximity to the spacecraft and the electrical units, quite different offsets may be found in orbit.

Much more effort has been invested in the determination of the FGM parameters in the deployed configuration. For this test step the spacecraft was moved to reference point RP3 which places FGM1 in the center of the facility. Except from this setup the same test procedure as described before was used.

Table 11.3-3: Parameters of FGM1, boom deployed

Scale factors in nT/EU (sensor temperature: 19°C)	CSC2 off		CSC2 on	
	S <sub>x</sub> =	1.001387	S <sub>x</sub> =	1.001608
	S <sub>y</sub> =	1.002305	S <sub>y</sub> =	1.002168
	S <sub>z</sub> =	1.002110	S <sub>z</sub> =	1.001967
Offsets	O <sub>x</sub> =	28.3 nT		
	O <sub>y</sub> =	19.9 nT		
	O <sub>z</sub> =	20.5 nT		
Misalignment angles	(X,Y) =	89.9741°		
	(X,Z) =	89.9384°		
	(Y,Z) =	89.9614°		

The determination of the instrument parameters of FGM2 is a little more difficult, since this magnetometer was out of the center during the calibration runs. We thus had to take the facility gradients into account. Estimates of the gradients have been derived from measurements at different positions. Corrected values are listed below.

Table 11.3-4: Parameters of FGM2, boom deployed

Scale factors in nT/EU (sensor temperature: 19°C)	CSC1 off		CSC1 on	
	S <sub>x</sub> =	0.999615	S <sub>x</sub> =	0.999836
	S <sub>y</sub> =	1.003836	S <sub>y</sub> =	1.003700
	S <sub>z</sub> =	1.001300	S <sub>z</sub> =	1.001157
Offsets	O <sub>x</sub> =	21.4 nT		
	O <sub>y</sub> =	8.1 nT		
	O <sub>z</sub> =	22.7 nT		
Misalignment angles	(X,Y) =	89.9353°		
	(X,Z) =	90.0296°		
	(Y,Z) =	89.9174°		

The uncertainty involved in our correction procedure is about  $\pm 5 \cdot 10^{-6}$  for the scale factor and  $\pm 1$  arcsec for the angles.

Comparing the obtained results with previous tests reveals that in particular the misalignment angles have been constant within arc seconds from the first calibration in March 1998 till present. This finding is valid for both FGM sensors. During the mission they may be considered as invariant which will reduce the number of free parameters for the in-flight calibration and enhance the significance of the other parameters.

The sets of parameters listed here may serve as the initial values for the interpretation of the FGM data during the early mission phase.

#### 11.4 Scalar Calibration of the FGMs

During the mission the FGM data will routinely be checked against the OVM readings. It has repeatedly been demonstrated that the so-called scalar calibration works perfectly with the CHAMP magnetometers (cf. [RD03]). A requirement for this kind of calibration is that magnetic field settings from different directions, well distributed over the sphere, are applied. During the mission the field distribution will be dominated by the dipolar shape of the geomagnetic field. Especially the Y component will experience only small deflections.

During the magnetic system test also three AOCS simulation runs were performed. During these runs the facility field was controlled by the AOCS Unit Tester generating the "real" magnetic environment for the simulated orbit phase and spacecraft orientation. Among others two orbits of normal operation in Fine Pointing Mode have been performed.

Data from these orbits shall be used to perform an in-flight scalar calibration. For comparison we have performed a scalar calibration with the spacecraft in the same position using a full set of well distributed field directions. Because of the gradients in the facility the obtained parameters are not good for data processing, but can be used to assess the quality of the in-flight calibration applied to the data of the AOCS simulation runs.

*Table 11.4-1: Results of the scalar calibration test  
(not good for data processing)*

	FGM1	FGM2
S <sub>x</sub>	1.001594 nT/EU	0.999818 nT/EU
S <sub>y</sub>	1.002139 nT/EU	1.003665 nT/EU
S <sub>z</sub>	1.001902 nT/EU	1.001099 nT/EU
O <sub>x</sub>	24.2 nT	15.2 nT
O <sub>y</sub>	19.4 nT	7.2 nT
O <sub>z</sub>	16.8 nT	18.9 nT
(X,Y)	89.9746°	89.9353°
(X,Z)	89.9315°	90.0246°
(Y,Z)	89.9614°	89.9170°

#### 11.5 Characteristics of the OVM

The OVM is regarded as the magnetic standard for the CHAMP mission. Therefore by definition no calibration is required. Nevertheless there are a few operational aspects which have to be taken into account.

In the stowed boom configuration the OVM does not function. The magnetic gradients from the spacecraft are too large to allow operating this instrument. It is therefore not possible to apply the in-flight calibration in this configuration.

If absolute magnetic field readings from OVM on CHAMP are expected, a number of influences of the spacecraft have to be taken into account.

1. The remanent magnetic field of the satellite can be taken into account, although it is rather small ( $<0.3$  nT) at the OVM and predominantly confined to the Y component (cf. Section 6.1).
2. The soft-magnetic parts of the satellite modify the field distribution. In section 6.1 we described how to compensate for that effects.
3. There is a cross-talk from the FGM sensors onto the OVM. The correction procedure has been described in [RD 03] section 7.3.
4. The magnetic fields emanating from the torquers have to be considered. The technique to eliminate them is given in equation (9.2-1).

In summary, we may state that the required absolute accuracy of 0.5 nT can comfortably be achieved by the OVM, if the above corrections are applied.

There has been a dedicated test to check whether the OVM produces interferences at the other magnetometers. Fortunately, there were no effects neither at the FGMs nor at the ASCs observed.

In case of a redundancy switch between the OBDH Main and Redundant the OVM is sometimes affected. As shown in Figure 11.5-1 the readings are then offset by about 1.5 nT. A power cycle of the OVM is required to get the instrument back to nominal operation.

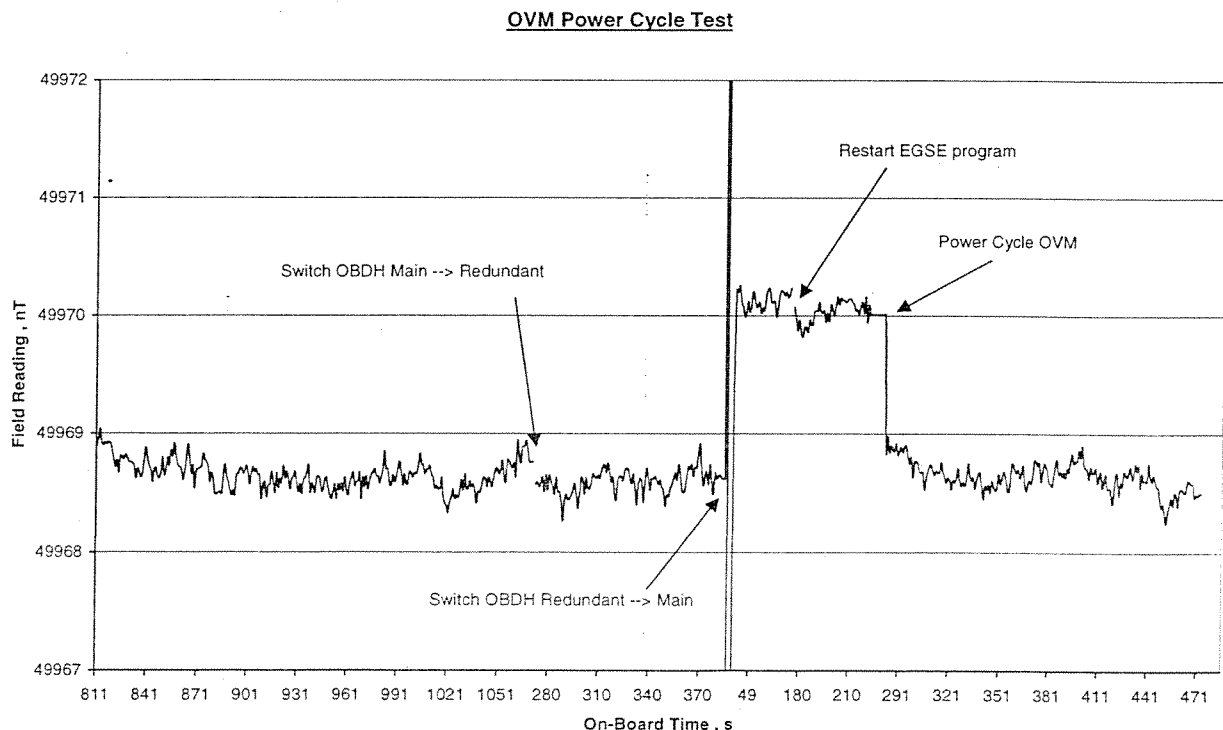



Figure 11.5-1 OVM offset after OBDH redundancy switch-over



	<b>CHAMP Magnetic Test Report</b>	Doc: CH-GFZ-TR-2000 Issue: 1.0 Date: 15.06.2000 Page: 49 of 51
---	---------------------------------------	---

Finally, the locking of the OVM on the ambient magnetic field was tested. The instrument safely locked after switch-on on the field which was changing at orbital rate during the AOCS test and tracked it without any problems.

When considering all the above mentioned effects the magnetic conditions on CHAMP are good enough to surpass the required absolute accuracy 0.5 nT and may even allow to make use of the high resolution of the OVM (50 pT) during the mission.

### 11.6 Timing of the Magnetic Field Readings

The magnetic test was also used to establish a precise dating of the magnetic field readings which includes all the delay times of the complete system. To maintain the full system precision requires to know the measurement time of the units of the magnetic field package to within a few milliseconds.

As a reference signal for this test we generated a square wave shaped magnetic field by the facility. The signal was high (+30 nT) for 8 sec and low (0 nT) for another 8 sec. The counter controlling the signal was driven by the 1-sec-pulse of a GPS receiver which guaranteed a high timing precision of the flanks. The spacecraft was operated according to the procedure steps "Timing and Synchronization" see [RD 01]. Data were taken by all three magnetometers.

Figure 11.6-1 shows an example of FGM 1 and 2 measurements at 50 samples per sec for a raising flank. The bottom panel displays the step response of the OVM. The flanks are not as steep as expected, but we can attribute the inflection point to the start of the second.

The basic features of magnetometer timing have already been discussed in section 8 of [RD 03]. A new element taking into account here for the dating of FGM readings is the time of the first sample ( $t_{\text{Sample}}$ ). In case of the OVM there are no changes.

Because of the rather gentle slope of the square wave, it is not possible to directly determine the dating of the FGM readings from a signal as shown in Figure 11.6-1. We decided to employ the Fourier analysis for this purpose. An interval of precisely 17 times the 16-sec period was used and the Fourier transform of the readings from the two FGMs and OVM was performed. Of interest are the results at the 16 sec period. Since the frequency response of the OVM is precisely known (cf. [RD 07]) and its internal cycle is rigidly fixed to the 1 Hz GPS synchronization pulse, we regard the results of this instrument as the timing reference. When comparing the phase angles derived by the various magnetometers one has to take into account deviation of the OVM filter from a linear phase response. At a 16-sec period wave the phase correction amounts to  $0.081^\circ$ . Considering furthermore the slight difference in the start time of the analyzed intervals, we find that FGM 1 and FGM 2 measurements have been taken 14.8 and 16.5 ms earlier, respectively, than indicated by their time stamp.

From this result we can derive the procedure for an absolute dating of the FGM readings:

#### 50 Hz mode

$$t_{\text{Meas.}} = t_{\text{Time Stamp}} - 1045 \text{ ms} + t_{\text{Sample}} + i \cdot 20 \text{ ms}; \text{ where } i \text{ runs from } 0 \text{ to } 49$$

#### 10 Hz mode

$$t_{\text{Meas.}} = t_{\text{Time Stamp}} - 1005 \text{ ms} + t_{\text{Sample}} + i \cdot 100 \text{ ms}; \text{ for } i = 0 \text{ to } 49$$

1 Hz mode

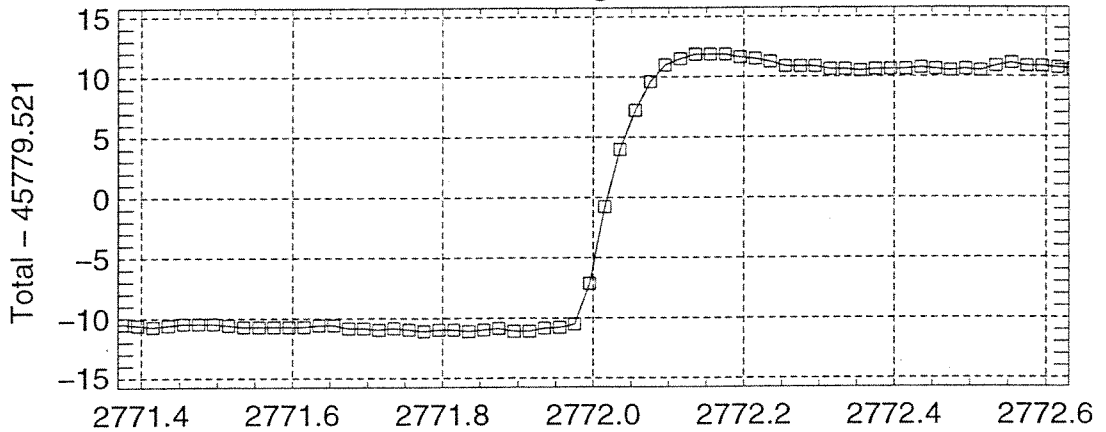
$$t_{\text{Meas.}} = t_{\text{Time Stamp}} - 555 \text{ ms} + t_{\text{Sample}}$$

For completeness, also the formula for the OVM is given here:

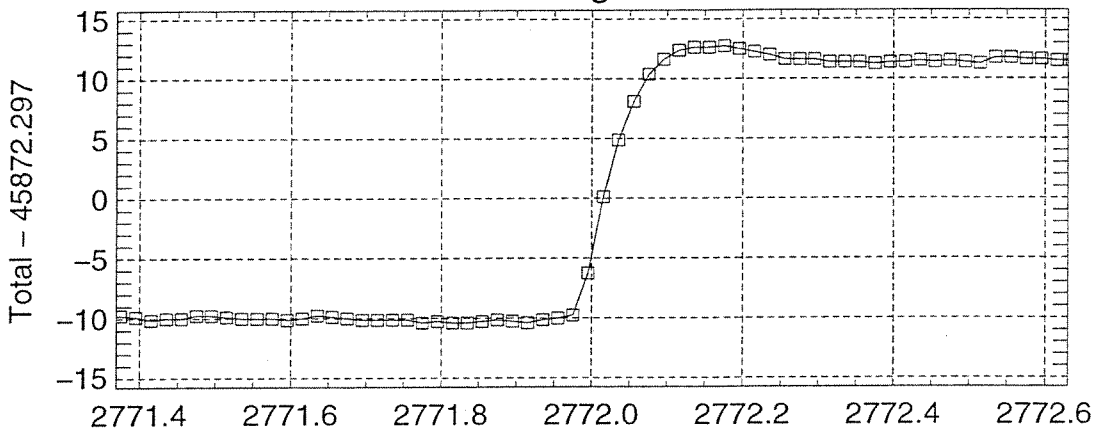
$$t_{\text{Meas.}} = t_{\text{Time Stamp}} - 860 \text{ ms}$$

The estimated uncertainty with respect to the time stamp is  $\pm 2$  ms.

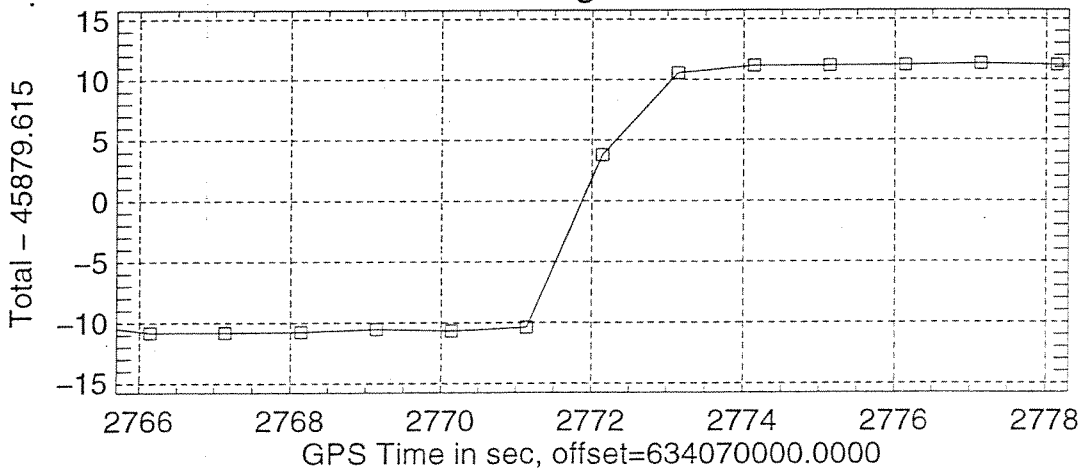
**FGM 1 Magnetic Test**



**FGM 2 Magnetic Test**



**OVM Magnetic Test**



---Report generated on Tue May 16 15:47:07 2000

Figure 11.6-1 Response of the magnetometers to a sudden field change at 2772 sec.